CO-RECEPTOR MEDIATED REGULATION OF T CELL RECEPTOR SIGNALLING IN NATURAL KILLER CELLS

by

Zeynep Sena Karahan

B.Sc., Genetics and Bioengineering, Yeditepe University, 2019

Submitted to the Institute for Graduate Studies in
Science and Engineering in partial fulfillment of
the requirements for the degree of
Master of Science

Graduate Program in Molecular Biology and Genetics

Boğaziçi University

2022

ACKNOWLEDGEMENTS

First and foremost, I would like to start by expressing my gratitude to my super supervisor, Assist. Prof. Tolga Sütlü, who has always been there for me, supported me and gave me brilliant advice whenever I needed it. He patiently guided me towards being a curious, ethical and unbiased scientist. I cannot thank him enough for welcoming me to his research group and making me a part of the Sütlü lab family. This has been a wonderful journey with his enthusiasm, immense knowledge and full support. I could not ask for a better mentor and advisor for my master's degree.

Besides my supervisor, I would also like to thank my jury member Prof. Dr Batu Erman who was always helpful with his insightful comments and hard questions during my academic work. I will always be appreciative of his wisdom and counsel.

I want to thank Prof. Dr Günnur Deniz for agreeing to join my thesis committee and for her time and advice regarding my thesis.

I would like to thank Emre Vatandaşlar from Medipol university for his help with the cell sorting and Prof. Dr Güher Saruhan Direskeneli from Istanbul University for the interleukin-2 supply. Without their assistance, I would not have been able to finish this thesis or obtain any data from which to draw a conclusion. I would also like to thank our collaborator Duru Lab and Asst. Prof. Adil Doğanay Duru for their help and support to the Sütlü lab.

I have always felt at home thanks to my Sütlü lab family. This journey would have been boring and uninspiring without you. I would like to thank all past and present members of Sütlü lab for being more than just a coworker; Ebru Zeynep Ergün, Elif Çelik, Cevriye Pamukcu, Mertkaya Aras, Gözde Özcan, Serra Özarı, Ayşegül Durgun, Bahar Orhan, Eren Can Ekşi, Betül Çakıcı, Elif Ayşenur Karay, Didem Özkazanç Ünsal, Alp Ertunga Eyüpoğlu, Pegah Zahedimaram, Ayhan Parlar, Aydan Saraç, Başak Özata. I was especially lucky because I have a science twin with me, Zeynep.

Zeynep and I have worked really closely during our master's degrees and I cannot thank her enough for always being there for me whether I need her or not. I could not imagine a better lab mate than her and I am forever grateful to her for making this fun and full of laughter. I will always remember and cherish our time together, and I will help others while thinking of our unconditional and loving solidarity. I love you. Special thanks to Elif for answering countless questions of mine patiently, always offering help and being the best flow queen one could ever see. Cevriye taught me everything she knows during the pandemic and I cannot thank her enough for the funniest memories. I will always remember and carry in my heart all of the sütlü lab members. Thank you for everything and the great memories! I hope we don't forget to dance and laugh together once in a while.

I would also like to thank Barış Can Mandacı, Ulduz Sobhi-Afshar and İlke Süder for their companionship and support during my time at Boğaziçi University. Likewise, I would also like to express my gratitude to Erman Lab, AKIL and YAMAN lab members for their help and support.

Last but not least, I am forever grateful for my caring, loving and supportive family. My warm and heartfelt thanks go to my parents, Necibe and Ali Karahan, for the tremendous support and love they had given to me. I could not survive this journey without my mom's delicious food and my dad's endless faith in me. My accomplishments and success are because they believed in me. I am thankful to my big sister Pervin Karahan for keeping me motivated and providing moral support.

Words cannot express my gratitude to my best friend Pofuduk and my dearest cat Patates. I could not have undertaken this journey without their unconditional love and support. They are the best life partners I could ever imagine and I'm beyond grateful to have them in my life. I love you.

ABSTRACT

CO-RECEPTOR MEDIATED REGULATION OF T CELL RECEPTOR SIGNALLING IN NATURAL KILLER CELLS

Antigen-specific cancer immunotherapy has been developing since the 1990s and showing promising results. T cell receptors (TCR) and Chimeric antigen receptors (CAR) are the most commonly used tools for modifying T cells with antigen-specific cytotoxicity. TCR-T cells have the mispairing problem caused by the endogenously produced TCR chains pairing with the ectopically delivered ones and creating T cells with unknown specificity. While NK cells contain all the necessary molecules for the downstream signalling pathway of TCR-CD3 mediated cytotoxicity they do not have the full TCR-CD3 complex. In order to overcome the mispairing problem in T cells, TCR and CD3 genes are used to modify NK cells instead of T cells. TCR-NK cells have shown promising cytotoxic effects against their target cells *in vitro* and *in vivo*, however their signalling mechanisms remain to be studied. CD8 coreceptors are known to increase the strength of the bond between TCR-CD3 and peptide-major histocompatibility complex (pMHC) and also aid the signalling cascade to begin. There are two types of CD8 chains, α and β. While T cells mostly utilise CD8$\alpha\beta$ heterodimers, some cells have the CD8$\alpha\alpha$ homodimer. This thesis aims to investigate the possible role of CD8 dimers in TCR-NK cells in order to optimise the TCR-NK cell cytotoxicity. Lentiviral constructs containing CD8 genes were delivered to TCR-NK cells. These TCR-NK-CD8 cells' cytotoxicity and antigen-specificity against the target cells were analysed with degranulation, cytokine secretion and real-time cell analysis assays. Western blot analysis was performed to observe the upregulated signalling pathways if present. Our results provide valuable data on the effect of CD8 coreceptors on TCR-NK cells.

ÖZET

DOĞAL ÖLDÜRÜCÜ HÜCRELERDE T HÜCRE RESEPTÖR SİNYALİZASYONUNUN KO-RESEPTÖR ARACILI DÜZENLENMESİ

Antijene özgü kanser immünoterapisi 1990'lardan beri gelişmekte ve umut verici sonuçlar vermektedir. T hücresi reseptörleri ve Kimerik antijen reseptörleri, T hücrelerini antijene özgü sitotoksisite ile modifiye etmek için en yaygın kullanılan araçlardır. TCR-T hücreleri, endojen olarak üretilen TCR zincirlerinin ektopik olarak verilenlerle eşleşmesinden ve bilinmeyen özgünlükte T hücreleri oluşturmasından kaynaklanan yanlış eşleşme sorununa sahiptir. NK hücreleri, TCR-CD3 aracılı sitotoksisitenin sinyal yolu için gerekli tüm molekülleri içerirken, tam TCR-CD3 kompleksine sahip değildirler. T hücrelerindeki yanlış eşleşme sorununun üstesinden gelmek için, T hücreleri yerine NK hücrelerini modifiye etmek için TCR ve CD3 genleri kullanılır. TCR-NK hücreleri, *in vitro* ve *in vivo* olarak hedef hücrelerine karşı umut verici sitotoksik etkiler göstermiştir, ancak bunların sinyal mekanizmaları henüz araştırılmayı beklemektedir. CD8 koreseptörlerinin, TCR-CD3 ve peptit-majör histo-uyumluluk kompleksi arasındaki bağın gücünü arttırdığı ve sinyalleme kaskadının başlamasına yardımcı olduğu bilinmektedir. α ve β olmak üzere iki tür CD8 zinciri vardır. T hücreleri çoğunlukla CD8$\alpha\beta$ heterodimerleri kullanırken, bazı hücrelerde CD8$\alpha\alpha$ homodimeri bulunur. Bu tez, TCR-NK hücre sitotoksisitesini optimize etmek için CD8 dimerlerinin TCR-NK hücrelerindeki olası rolünü araştırmayı amaçlamaktadır. CD8 genleri içeren lentiviral yapılar, TCR-NK hücrelerine verildi. Bu TCR-NK-CD8 hücrelerinin hedef hücrelere karşı sitotoksisitesi ve antijen spesifikliği, degranülasyon, sitokin salgılanması ve gerçek zamanlı hücre analizi deneyleriyle analiz edildi. Yukarı regüle edilmiş sinyal yollarını gözlemlemek için Western blot analizi yapıldı. Sonuçlarımız, CD8 koreseptörlerinin TCR-NK hücreleri üzerindeki etkisi hakkında değerli veriler sağlar.

TABLE OF CONTENTS

ACKNOWLEDGEMENTS . . . iii
ABSTRACT . . . v
ÖZET . . . vi
LIST OF FIGURES . . . x
LIST OF TABLES . . . xiv
LIST OF SYMBOLS . . . xvii
LIST OF ACRONYMS/ABBREVIATIONS . . . xviii
1. INTRODUCTION . . . 1
1.1. The Immune System . . . 1
1.2. Cytotoxic Lymphocytes of the Immune System . . . 3
1.2.1. T Cells . . . 4
1.2.1.1. Description and Origin . . . 4
1.2.1.2. Subtypes . . . 5
1.2.1.3. T Cell Receptors and Co-receptors . . . 6
1.2.1.4. Target Recognition . . . 8
1.2.1.5. T Cell Activation . . . 9
1.2.2. Natural Killer Cells . . . 11
1.2.2.1. Description and Origin . . . 11
1.2.2.2. Subtypes . . . 12
1.2.2.3. Effector Mechanisms . . . 13
1.2.3. Cellular Immunotherapy of Cancer . . . 14
1.2.4. TCR-T and CAR-T Cells . . . 17
1.2.5. TCR-NK Cells . . . 18
2. AIM . . . 21
3. MATERIALS AND METHOD . . . 22
3.1. Materials . . . 22
3.1.1. Chemicals . . . 22
3.1.2. Equipments . . . 22
3.1.3. Buffers and Solutions . . . 22

3.1.4. Growth Media . . . 23
3.1.5. Enzymes . . . 24
3.1.6. Antibodies . . . 25
3.1.7. Commercial Kits . . . 26
3.1.8. Bacterial Strains . . . 26
3.1.9. Mammalian Cell Lines . . . 26
3.1.10. Plasmids and Oligonucleotides . . . 27
3.1.11. DNA Ladder . . . 30
3.1.12. Protein Ladder . . . 30
3.1.13. DNA Sequencing . . . 30
3.1.14. Software, Computer-based Programs and Websites . . . 31
3.2. Method . . . 31
3.2.1. Bacterial Cell Culture . . . 31
3.2.2. Mammalian Cell Culture . . . 33
3.2.3. Cloning of T Cell Receptors and Co-receptors . . . 34
3.2.3.1. LeGO.DGE.IRES.puro Cloning . . . 34
3.2.3.2. LeGO-CD8α-iT2p Cloning . . . 38
3.2.3.3. LeGO-CD8β-iT2p Cloning . . . 41
3.2.4. Production of Lentiviral Vectors . . . 45
3.2.5. Lentiviral Transduction of NK-92 Cells . . . 46
3.2.6. Flow Cytometry . . . 46
3.2.7. Analysis of NK Cell Cytotoxicity by Xcelligence RTCA . . . 47
3.2.8. Analysis of NK Cell Degranulation . . . 48
3.2.9. Intracellular TNF-α and IFN-γ Staining . . . 48
3.2.10. Western Blot Analysis . . . 49
3.2.11. Statistical Analysis . . . 49
4. RESULTS . . . 50
4.1. Cloning of T Cell Receptors and Co-receptors . . . 50
4.1.1. LeGO.DGE.IRES.puro Cloning . . . 50
4.1.2. LeGO.CD8α.iT2p Cloning . . . 51
4.1.3. LeGO.CD8β.iT2p Cloning . . . 52

4.2. Production of Lentiviral Vectors 53
4.3. Cell Surface Assembly of TCR Complex in NK Cells 54
4.3.1. Genetic Modification of NK-TyrTCR Cell Line with CD3 Chain Genes 54
4.3.2. Genetic Modification of NK-TyrTCR-DGEip Cell Line with Coreceptor Genes 55
4.4. Triggering and Specificity of CD8-expressing TCR-NK Cells 57
4.4.1. Degranulation of CD8-expressing TCR-NK Cells 57
4.4.2. Cytotoxic Activity of CD8-expressing TCR-NK Cells 58
4.4.3. TNF-α and IFN-γ secretion of CD8-expressing TCR-NK Cells . 62
4.4.4. Protein Analysis of CD8-expressing TCR-NK Cells 66
5. DISCUSSION 68
6. REFERENCES 73
APPENDIX A: Chemicals Used in This Study 84
APPENDIX B: Equipments Used in This Study 86
APPENDIX C: ADAPTATIONS 88
APPENDIX D: DNA Ladder Used in This Study 89
APPENDIX E: Protein Ladder Used in This Study 90
APPENDIX F: Plasmid Maps 91

LIST OF FIGURES

Figure 1.1. The schematic diagram showing the cells of the immune system. (Adapted from "Stem Cell Differentiation from Bone Marrow" by BioRender.com.) 2

Figure 1.2. Different modes of recognition by T and NK cells via MHC. 3

Figure 1.3. Structure of a T cell receptor. 6

Figure 1.4. Antigen processing and presentation for different MHC classes. . . 9

Figure 1.5. Schematic representation of T cell activation. 11

Figure 1.6. NK Cell subsets with different expression patterns of receptors. . . 12

Figure 1.7. Schematic diagram of adoptive cell therapy. 16

Figure 1.8. Different types of antigen specific immunotherapy. 17

Figure 1.9. Schematic representation of mispairing problem in TCR-T cell immunotherapy. 18

Figure 4.1. Gel image of colony PCR result from LeGO-DGE-IRES-puro colonies. 50

Figure 4.2. Confirmation of LeGO-DGE-IRESpuro cloning with control digestion. 51

Figure 4.3. Gel image of colony PCR result from LeGO-CD8α-iT2p colonies. . 51

Figure 4.4. Confirmation of LeGO-CD8α-iT2p cloning with control digestion. . 52

Figure 4.5. Gel image of colony PCR result from LeGO-CD8β-iT2p colonies. . 52

Figure 4.6. Confirmation of LeGO-CD8β-iT2p cloning with control digestion. . 53

Figure 4.7. Schematic representation of lentiviral constructs used in this study. 53

Figure 4.8. Genetic modification process of NK92-TyrTCR cells with LeGO-DGE-IRES-puro lentiviral vector and sorting with puromycin selection results on flow cytometry showing CD3 expression. 55

Figure 4.9. Genetic modification process of NK92-TyrTCR-DGE-IRES-puro cells with CD8 lentiviral vectors and FACS sorting results on flow cytometry. 56

Figure 4.10. Degranulation of NK92-TCR-DGE-CD8 cells. 58

Figure 4.11. Degranulation of NK92-TCR-DGE-CD8 cells at different time points. 58

Figure 4.12. Real-time cell analysis of different effector cells against A375 and A375Tyr cells. 59

Figure 4.13. Cell index measurements at different time points which were baseline-corrected to no effector cell indexes. E:T = 1:1. 60

Figure 4.14. Real-time cell analysis of different effector cells against A375 and A375Tyr cells. E:T = 0.1:1. 60

Figure 4.15. Cell index measurements at different time points which were baseline-corrected to no effector cell indexes. E:T = 0.1:1. 61

Figure 4.16. Real-time cell analysis of different effector cells against A375 and A375Tyr cells. E:T = 0.3:1. 61

Figure 4.17. Cell index measurements at different time points which were baseline-corrected to no effector cell indexes. E:T = 0.3:1. 62

Figure 4.18. TNFα secretion levels of stimulated TCR-NK cells represented with a bar graph. 62

Figure 4.19. IFNγ secretion levels of stimulated TCR-NK cells represented with a bar graph. 63

Figure 4.20. Flow cytometry analysis of TNFα secretion levels released by effector cells against A375Tyr cells. 64

Figure 4.21. Flow cytometry analysis of IFNγ secretion levels released by effector cells against A375Tyr cells. 65

Figure 4.22. Phospho-PLCγ1 expression levels of effector cells stimulated with target cells for 1 hour. 66

Figure 4.23. Phospho-Erk1/2 and total Erk expression levels of effector cells stimulated with target cells for 1 hour. 67

Figure D.1. DNA ladder used in this study. 89

Figure E.1. Protein ladder used in this study. 90

Figure F.1. The vector map of LeGO-iT2p. 91

Figure F.2. The vector map of LeGO-iG2p. 92

Figure F.3. The vector map of LeGO-DGEiTCR. 92

Figure F.4. The vector map of LeGO-DGE-IRESpuro. 93

Figure F.5. The vector map of pCI-neo-CD8α 93

Figure F.6. The vector map of pcDNA3.1-CD8βM-1. 94

Figure F.7. The vector map of LeGO_CD8α_iT2p. 94

Figure F.8. The vector map of LeGO_CD8β_iT2p. 95

Figure F.9. The vector map of pMDLg/pRRE 95

Figure F.10. The vector map of pRSV-Rev. 96

Figure F.11. The vector map of pCMV-VSV-G. 96

LIST OF TABLES

Table 3.1. List of Enzymes. 24

Table 3.2. List of Antibodies. 25

Table 3.3. List of Commercial kits. 26

Table 3.4. List of Plasmids 27

Table 3.5. List of Oligonucleotides 29

Table 3.6. List of software and websites. 31

Table 3.7. PCR of puromycin gene from LeGO-iG2puro. 34

Table 3.8. Condition of PCR for puromycin extraction. 35

Table 3.9. Digestion of puromycin insert. 35

Table 3.10. Digestion of LeGO-DGE-IRES-TCR backbone vector. 36

Table 3.11. CIP treatment of the backbone vector. 36

Table 3.12. Ligation reaction of backbone and insert. 37

Table 3.13. Colony PCR for colonies picked from transformation plates. 37

Table 3.14. Condition of Colony PCR. 38

Table 3.15. Digestion of pCI-neo-CD8α vector. 38

Table 3.16. Digestion of LeGO-iT2puro vector. 39

Table 3.17. CIP treatment of the backbone vector. 39

Table 3.18. Ligation reaction of backbone and insert. 40

Table 3.19. Colony PCR for colonies picked from transormation plates. 40

Table 3.20. Condition of Colony PCR. 41

Table 3.21. PCR for CD8β insert. 42

Table 3.22. Condition of PCR. 42

Table 3.23. Digestion of CD8β insert. 43

Table 3.24. Digestion of LeGO-iT2p backbone vector. 43

Table 3.25. CIP treatment of the backbone vector. 44

Table 3.26. Ligation reaction of backbone and insert. 44

Table 3.27. Colony PCR for colonies picked from transormation plates. 45

Table 3.28. Condition of Colony PCR. 45

Table 4.1. Titration table of lentiviruses. 54

Table 4.2. Results of the lentiviral transductions and selection/sorting 57

Table A.1. Chemicals used in this study. 84

Table B.1. Equipments used in this study. 86

LIST OF SYMBOLS

g	Gram
L	Liter
M	Molar
mL	Mililiter
mM	Milimolar
ng	Nanogram
α	Greek letter alpha
β	Greek letter beta
δ	Greek letter delta
γ	Greek letter gamma
ϵ	Greek letter epsilon
κ	Greek letter kappa
ζ	Greek letter zeta
μg	Microgram
μl	Microliter
μM	Micromolar
μm	Micrometer

LIST OF ACRONYMS/ABBREVIATIONS

ACT	Adoptive Cell Therapy
APC	Antigen Presenting Cell
APC	Allophycocyanin
bp	Basepair
BV	Brilliant Violet
CAR	Chimeric Antigen Receptor
CI	Cell Index
CO_2	Carbon Dioxide
CTL	Cytotoxic T Lymphocyte
DC	Dendritic Cell
ddH_2O	Distilled Water
DMEM	Dulbecco's Modified Eagle Medium
DMSO	Dimethylsulfoxade
DNA	Deoxyribonucleic Acid
E.coli	Escherichia Coli
EDTA	Ethylenediaminetetraacetic Acid
FACS	Fluorescence Activated Cell Sorting
FBS	Fetal Bovine Serum
GFP	Green Fluorescent Protein
GvHD	Graft Versus Host Disease
HEPES	4-(2-hydroxyethyl)-1-piperazineethanesulfonic Acid
HLA	Human Leukocyte Antigen
IFN	Interferon
IgG	Immunoglobulin G
IL	Interleukin
IRES	Internal Ribosome Entry Site
ITAM	Immunoreceptor Tyrosine-based Activation Motif
ITIM	Immunoreceptor Tyrosine-based Inhibition Motif

Kd	Kilodalton
KIR	Killer-cell Immunoglobulin-like Receptor
LB	Luria Broth
LeGO	Lentiviral Gene Ontology Vectors
LFA	Lymphocyte Function-associated Antigen
LTR	Long Terminal Repeat
mAb	Monoclonal Antibody
MHC	Major Histocompatibility Complex
MOI	Multiplicity Of Infection
NK	Natural Killer
NKT	Natural Killer T cells
NEAA	Non-essential Amino Acid
OXO	(5Z)-7-Oxozeaenol
PAMP	Pathogen Associated Molecular Pattern
PBMC	Peripheral Blood Mononuclear Cell
PBS	Phosphate Buffered Saline
PCR	Polymerase Chain Reaction
PD-1	Programmed Cell Death Protein 1
PFA	Paraformaldehyde
PIPES	Piperazine-N,N′-bis (2-ethanesulfonic acid)
PLC-γ-1	Phospholipase Gamma 1
PMA	Phorbol 12-myristate 13-acetate
Puro	Puromycin
RAG	Recombination Activating Gene
RIPA	Radioimmunoprecipitation Assay
RNA	Ribonucleic Acid
Rpm	Round Per Minute
RPMI	Roswell Park Memorial Institute
RT	Room Temperature
RTCA	Real Time Cell Analysis
SDS-PAGE	Sodium Dodecyl Sulfate Polyacrylamide Gel Electrophoresis

SFFV	Spleen Focus Forming Virus
TAA	Tumor-associated Antigen
TBE	Tris Boric Acid EDTA
TCR	T Cell Receptor
tdTomato	Tandem Dimer Tomato
TNF	Tumor Necrosis Factor
TRAIL	TNFα-Related Apoptosis-Inducing Ligand
Tyr	Tyrosinase
VSV-G	Vesicular Stomatitis Virus G
WB	Western Blot
WT	Wild Type
ZAP-70	Zeta-associated Of 70 Kd Tyrosine kinase

1. INTRODUCTION

1.1. The Immune System

When the body is under threat of either an external agent or an internal disruption, the immune system intervenes. The immune system consists of various effector cells and molecules that together defend the body (Figure 1.1). The innate immune system is the first one to act upon pathogens whereas the adaptive immune system requires time to be activated since it works in an antigen-specific way (Medzhitov & Janeway, 2000). Dendritic cells, natural killer cells, eosinophils, neutrophils, mast cells and macrophages belong to the innate immune system and they become activated in case there is an infection and an inflammatory response caused by this. The activation takes place through the pathogen-associated molecular patterns (PAMPs) being recognised by the pattern recognition receptors (PRRs) of the innate immune system. These cells' main duty is to eliminate the infection. However, in some cases, they are unable to do so where adaptive immune system activation is required (Janeway & Medzhitov, 2002).

Dendritic cells (DCs) play an important role in the activation of the adaptive immune system since they present microbial antigens to the T cells. At the infection site, DCs identify and phagocytose the microorganisms or their parts that cause the infection. Then they proceed to a peripheral lymphoid organ where T cells can be activated via antigen presentation (Trombetta & Mellman, 2005). All proteins in a cell are processed and presented as small peptides on the major histocompatibility complexes (MHC) on the surface of nucleated cells. They provide identification for the cells and make it possible for T cells to detect if there are any foreign molecules in the cell (Neefjes et al., 2011). The recognition mechanism of T cells depends on peptide-MHC (pMHC) complexes and the quality of the bond between TCRs and pMHCs determines the answer of T cells. If there are any foreign peptides on the MHCs then T cells are activated (Santana & Esquivel-Guadarrama, 2006).

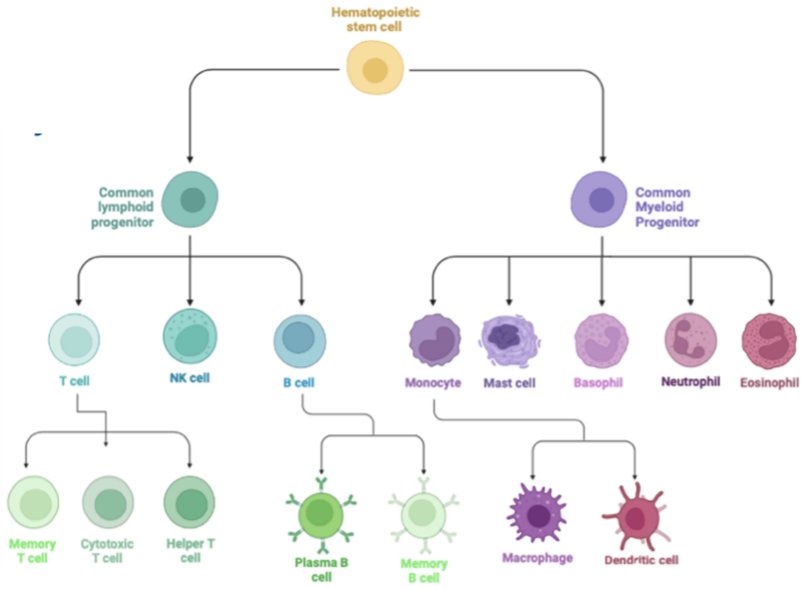

Figure 1.1. The schematic diagram showing the cells of the immune system. (Adapted from "Stem Cell Differentiation from Bone Marrow" by BioRender.com.)

While some of the activated T cells migrate to help other phagocytic cells at the site of infection, other T cells rest in the lymphoid organ and aid the activation and maturation of B cells. Soluble antibodies are produced by B cells and they specifically target the invading microorganisms. Once T and B cells remove the pathogens from the host, a small amount of these antigen specific lymphocytes remain in the body in order to become memory cells for fighting future invasions better (Alberts B. et al., 2002).

Innate and adaptive immunity works together to fight infections. Without the innate immunity handling the pathogens in the first few days, the adaptive immunity would not have enough time to develop specific fighters, T and B cells, for the invasion. On the other hand, innate immunity is not enough for all the invaders and requires adaptive immunity for a better defense. Thus, adaptive and innate immune responses are considered two integrated parts of the immune system (Medzhitov R. & Janeway CA, 1997).

1.2. Cytotoxic Lymphocytes of the Immune System

Since there are different routes and types of invaders there are also different types of recognition ways and responses against them in the immune system. Natural killer (NK) cells and CD8+ T cells are the major cytotoxic lymphocytes for viral infections. Even though they belong to separate arms of the immune system, they both originate from a common lymphoid progenitor together with B cells. NK and cytotoxic T cells both utilize perforin and granzymes as their killing mechanism and both use cytokine signals for activation such as interleukin-12 (IL-12) and type-1 interferons (Sun & Lanier, 2011). The way NK cells and cytotoxic T cells are distinguished from each other is through their recognition mechanisms. While T cells directly bind to pMHC complexes and control the identity of both of them, NK cells only check the presence of MHCs. Self-MHC complexes send inhibitory signals to NK cells therefore their activation is stopped. On the other hand, T cells are only activated if the peptide presented in the MHC/peptide complex is foreign (Figure 1.2) (Murphy et al., 2017).

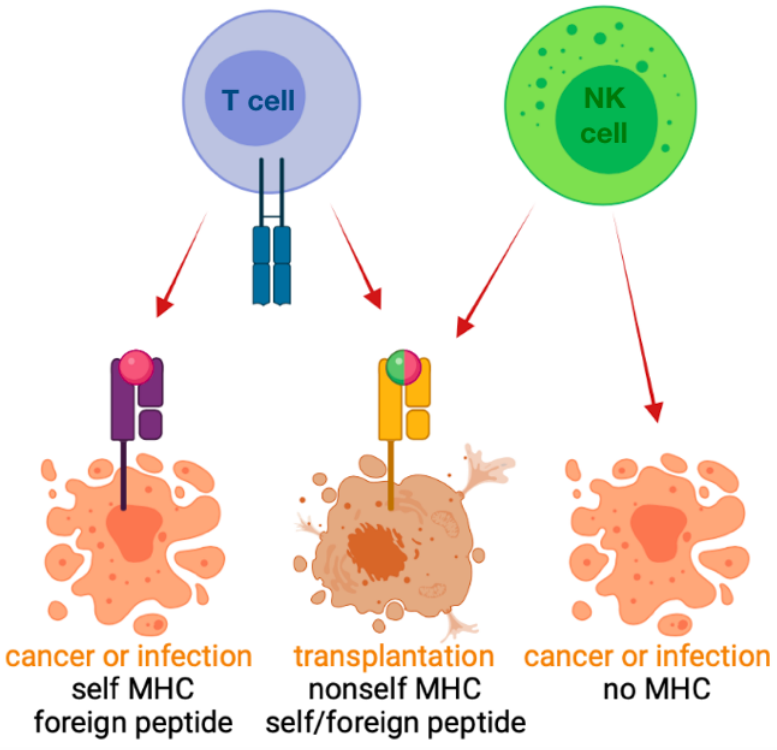

Figure 1.2. Different modes of recognition by T and NK cells via MHC.

1.2.1. T Cells

1.2.1.1. Description and Origin. Jacques Miller, the Australian immunologist, was the one who found out the thymus was responsible for producing an important type of lymphocyte essential for the immune response in the 1960s. After the discovery of two lines of lymphocytes present in the body, (M. D. Cooper, 2002) it was also observed that bone marrow-derived cells (B cells) require thymus-derived cells to produce antibodies. These cells were later identified as T helper cells, which are a subset of the T lymphocytes (J. F. A. P. Miller, 2002).

There are several developmental steps for T cells to mature starting with T cell lineage commitment rather than B cell lineage. Multipotent hematopoietic stem cells in the bone marrow are precursors of both B and T cells. While B cells complete their maturaion in the bone marrow, T cell maturation occurs in the thymus. The hematopoietic stem cells that leave the bone marrow and migrate to the thymus receive signals from the thymic epithelial cells which are transduced through the Notch1 receptor on the cell surface. Notch1 signalling drives the T cell lineage commitment over B cell lineage and it also plays a role in the selection of the T cell receptor (TCR) chain lineage which can be $\alpha\beta$ or $\gamma\delta$ (Deftos & Bevan, 2000; Murphy et al., 2017).

T cells express receptors (TCRs) that recognise pMHC complexes presenting foreign antigens. The genes producing these receptors are somatically rearranged and every T cell has a TCR recognizing a unique and specific antigen. It is also possible to generate an autoreactive TCR that can be detrimental to the body, however, these self-reactive cells are mostly detected and killed in the thymus by the negative selection process. Although there are several checkpoints during the T cell development to ensure the TCR produced is functional and not harmful, some T cells might escape this selection process and cause autoimmune diseases (Robey & Fowlkes, 1994; Thome et al., 2014).

T lymphocytes are also responsible for immunological memory and self-tolerance. Since memory T cells are able to recognize a pathogen encountered early in a lifetime,

they provide lifelong protection. While naïve T cells, which are newly emerged from the thymus, are responsive to new antigens, activated cytotoxic T cells can readily fight an invasion. These different types of T cells are scattered across the body and vary during different life stages and invasions (Kumar et al., 2018; Thome et al., 2014).

1.2.1.2. Subtypes. T cells go through a series of differentiation steps in the thymus. These changes can be followed via different expression patterns of TCRs and the co-receptor proteins CD4 and CD8. Different combinations of receptor chains and cell surface proteins result in different T cell subpopulations and they all have specific functions in the body and secrete characteristic cytokines. Early in T cell development, there are two distinct lineages according to different types of T cell receptor chain dimers which are α:β and γ:δ T cells. The γ:δ T cells that makeup approximately 10% of thymocytes in the body reside mostly in the mucosal and epithelial sites after leaving the thymus. They are considered a component of the innate immune system since they can act rapidly once activated. CD4 and CD8 co-receptor expressions are non-existent in these cells (Murphy et al., 2017).

On the other hand, α:β T cells have the expression of both CD4 and CD8 co-receptors at the beginning of their maturation in the thymus and at this stage, they are called double-positive (DP) thymocytes. The DP cells that have functional α:β TCRs, which are capable of engaging with the self-MHC molecules, are subjected to positive selection where they receive survival signals to continue their development into mature T cells. The ones that cannot recognize the self MHCs or have high reactivity to self pMHC complexes and would cause autoimmune diseases are negatively selected and killed in the thymus. After the positive selection step, DP cells become either CD4+ single-positive (SP) helper T cells or CD8+ SP cytotoxic T cells (Singer et al., 2008). CD4+ T cells also differentiate into subpopulations with different cytokine profiles, which are T helper cells (Th), regulatory T cells (Treg) and follicular helper T cells (Tfh) (Golubovskaya & Wu, 2016).

There is also another T cell subpopulation that has an invariant TCR chain (Vα24/Jα18/β11) known as natural killer T (NKT) cells. They target foreign lipids and glycolipids presented in the MHC-I-like protein CD1d and can act upon activation faster than the conventional T cells by producing large amounts of IL-4 and IFN-γ. They are recognized as a bridge between innate and adaptive immunity since they have both NK cell and T cell features (Spada et al., 1998).

1.2.1.3. T Cell Receptors and Co-receptors. Six chains of CD3 subunits and two T cell receptor (TCR) chains make up the TCR complex on the surface of T cells (Figure 1.3). The antigen recognition in T cells is operated through the interaction between TCRs and pMHC of antigen-presenting cells such as dendritic cells and macrophages. TCRs were first identified at the beginning of the 1980s via various studies (Gaud et al., 2018; Samelson et al., 1988).

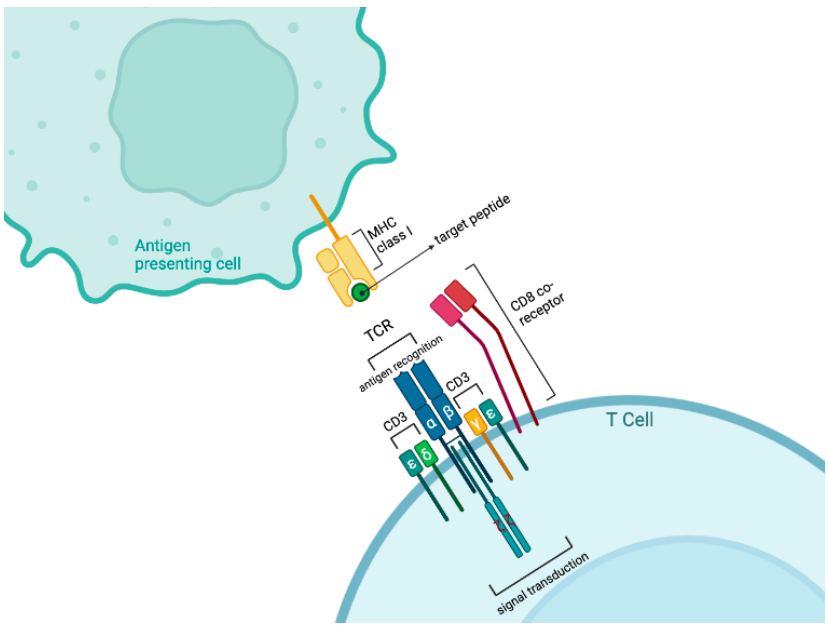

Figure 1.3. Structure of a T cell receptor.

Approximately 90% of the TCR heterodimers are α:β and both chains have an immunoglobulin(Ig)-like extracellular variable (V) and constant (C) domain where the antigen specificity is provided by the variable domain. The V domains are encoded by gene segments called V, D and J which require somatic recombination before they

construct the V domain. This VDJ recombination occurs during the T cell development and determines the antigen specificity of a T cell. This results in a vast T cell diversity and thus the T cells are capable of targeting different kinds of antigens on MHCs (Desch et al., 1996; Rossjohn et al., 2015).

Three dimers of CD3 chains are crucial for TCR signalling and localization on the surface, δε and γε heterodimers and ζζ homodimers. They are essential for signal transduction when the TCR chain binds to a pMHC complex with high affinity. This binding must be strong and stable enough to trigger the signal transduction and co-receptors (CD8 and CD4), play a role in a more stable TCR-pMHC binding. While CD4 receptors consist of a single polypeptide chain, CD8 is present either as a heterodimer (CD8αβ), which is exclusively expressed on cytotoxic T cells or as a homodimer (CD8αα). (Shah et al., 2021) γδ T cells and NK cells have the expression of CD8αα homodimer. Although the binding affinities of CD8 dimers to pMHC-I are similar, it has been shown that the CD8αβ has stronger functional activity compared to CD8αα due to the function of CD8β. It has been demonstrated that CD8β enhances the co-receptor and pMHC interaction with its ectodomain while also helping the lipid raft association with its intracellular domain by getting palmitoylated (Cheroutre & Lambolez, 2008; Kern et al., 1999).

Co-receptors are also important regulators during thymocyte development, ensuring the MHC class preference of the T cells. The cytotoxic CD8+ T cells are MHC class I restricted and since all nucleated cells have MHC-I on them, CD8+ T cells are able to scan and act on all cells with a nucleus that are infected. However, only professional antigen-presenting cells (APC) with pMHC-II are able to activate CD4+ helper T cells, and this aids in the activation of B cells. (Figure 1.4.) (Mørch et al., 2020).

The cytoplasmic tail of both CD4 and CD8 is important for TCR activation since they are associated with Lck. This Src family kinase phosphorylates the immunoreceptor tyrosine-based activation motifs (ITAMs) which are based in the intracellular domains of CD3 subunits and initiate the TCR activation by triggering downstream

signalling pathways. However, it has been shown that the co-receptors are not indispensable for this since co-receptor-independent T cell activation has also been observed (Mørch et al., 2020; Schilhammo et al., 1993).

1.2.1.4. Target Recognition. The VDJ recombination that produces the variable domain of TCR α and β chains results in complementarity-determining region (CDR) loops in the TCR stucture. There are 3 loops in each chain, making up 6 loops in total and they are essential for pMHC complex recognition. While CDR1 and CDR2 are interacting with the MHC, CDR3 binds to the peptide presented on that MHC (Sharon et al., 2016; Wong et al., 2019). There are two types of MHC classes in humans, class I and class II, sharing a similar general structure but differing in their subunit assembly. While they both consist of four subunits making up two polypeptide chains, only one polypeptide chain of MHC-I spans the membrane. On the other hand, MHC-II has two chains spanning the membrane and a more open peptide-binding cleft compared to MHC-I. The peptide and MHC complex should be stable enough for TCRs to bind and detect any foreign peptides. The way the peptides are bound to MHC molecules as an integral part is important for appropriate interaction with T cells and MHC molecules are not stable when they do not have a peptide inside of their cleft (Murphy et al., 2017).

While the expression of MHC-I is present in all nucleated cells in the body, only the APCs (dendritic cells, B lymphocytes and macrophages) have the expression of MHC-II. As aforementioned, αβ T cells are subdivided into CD4+ and CD8+ T cells. The main difference between these cells is that they recognize different MHC classes and function with distinct outcomes. The proteasome processes foreign proteins produced by infected cells during intracellular infections caused by viruses, and the resultant peptides are then displayed on MHC-I molecules that are recognized by cytotoxic CD8+ T lymphocytes (Figure 1.4.). CD8+ T cells, scan the peptides on MHC-I molecules and are able to exert their cytotoxic effects (Reeves & James, 2017; Trombetta & Mellman, 2005).

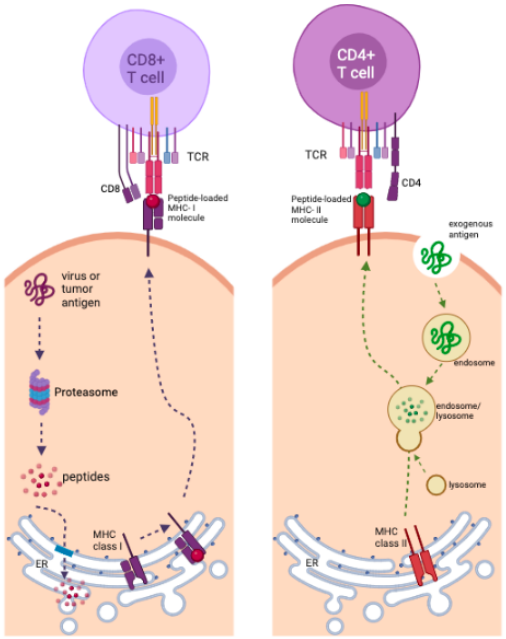

Figure 1.4. Antigen processing and presentation for different MHC classes.

On the other hand, the source of the MHC-II ligands is endogenous proteins which may be picked up through phagocytosis, processed and presented on MHC-II molecules by professional APCs that exclusively express MHC Class II genes (Figure 1.4.) CD4+ helper T cells recognise pMHC-II complexes on APCs and upon activation, they help other effector cells to be activated. If they interact with a pMHC-II on B cells, they secrete cytokines that help B cells to produce appropriate antibodies for the foreign peptide that eliminates the bacterial infection (Jensen, 2007; Trombetta & Mellman, 2005; Vyas et al., 2008).

1.2.1.5. T Cell Activation. The cytotoxic effect of primed CD8+ T cells might be observed within a short time upon binding to the pMHC-I complex. However, the initial priming of naive CD8+ and CD4+ T cells requires a longer time. In order to transduce the signal in the T cell and upregulate the pathways that activate the proliferation of T cells that are specific to the pathogen, a longer and more stable interaction is required. The affinity between TCRs and pMHC complexes is very low, nevertheless, there are several mechanisms to maintain this interaction long enough to induce the activation of T cells (Xu et al., 2020). When a TCR binds to an agonist

ligand on MHC, the surface molecules are clustered in the contact area, forming an immunological synapse (IS) and increasing the interaction duration while the molecules negatively affecting the adhesion of two cells are excluded from this region. Lymphocyte function-associated antigen 1 (LFA-1) is also clustered at the synapse and increases the adhesion of two cells. The cytoskeleton of the T cells is reorganized in order to slow down their migration since they move rapidly while scanning the cells (Kupfer & Singer, 1989; M. J. Miller et al., 2002).

As mentioned above, CD8 and CD4 coreceptors bind to MHC-I and MHC-II respectively and increase the stability of TCR-pMHC complex interaction. They are also associated with Lck on their cytoplasmic tails and this increases the phosphorylation of ITAMs on the CD3 chains (Gascoigne et al., 2010). After the adequate phosphorylation of ITAMs by Src-family kinases Lck and Fyn, the signalling cascade starts in the T cell. ZAP-70 is recruited since the phosphorylated ITAMs are docking sites for their SH2 domains and it phosphorylates LAT and SLP-76 adaptor proteins after it is phosphorylated and activated by Lck (Mørch et al., 2020). These adaptor proteins are linked with Gads, another adaptor protein, and generate a protein complex called LAT:Gads:SLP-76 which plays an essential role in T cell activation. PI 3-kinase enzyme is also recruited and activated after the ZAP-70 activation. After these cascades, T cell activation is divided into four branches such as (i) activation of phospholipase C-γ (PLC-γ), (ii) activation of Akt, (iii) activation of Vav and (iv) recruitment of the adaptor protein ADAP where they all have various outcomes (Figure 1.5.).

The activation of many transcription factors by PLC-activation results in fast T cell proliferation and the production and release of a number of cytokines and chemokines. The nuclear factor of activated T cells (NFAT) transcription factors are activated through the influx of calcium entry into the cytosol induced by PLC- γ. The mitogen-activated protein kinase (MAPK) cascade is another pathway that is activated by PLC- γ and results in the activation of transcription factors such as AP-1 by the extracellular signal-related kinase (Erk).

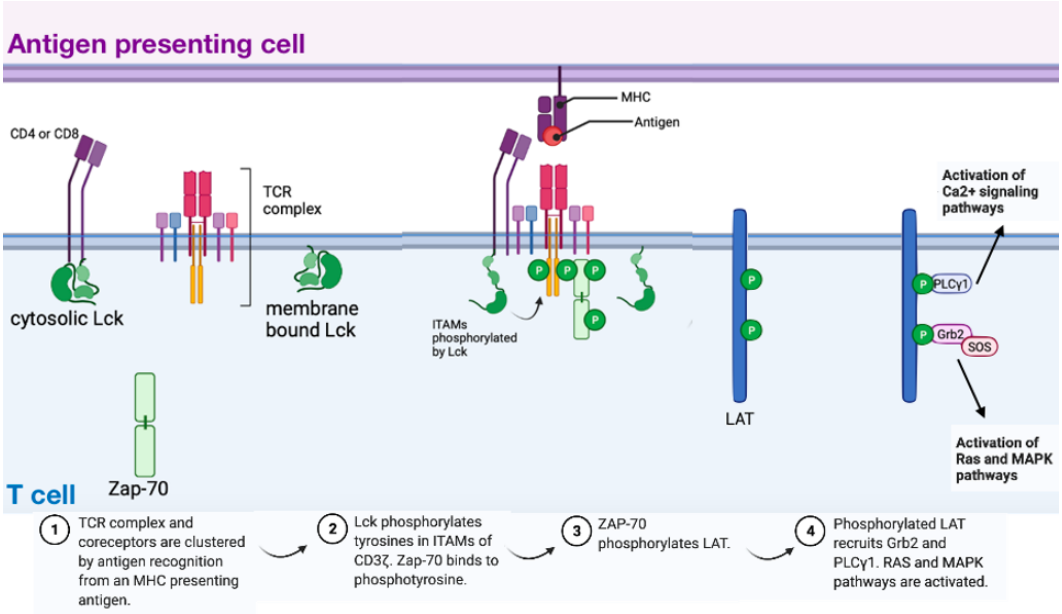

Figure 1.5. Schematic representation of T cell activation.

Another transcription factor family that is activated through PLC- γ is NFκB. As an outcome of activation of these transcription factors, IL-2 is produced which is important for proliferation and differentiation of T cells. Activation of Akt protein results in increased metabolic activity that the activated T cell requires. Akt activates the mammalian target of rapamycin (mTOR) pathway where macromolecular biosynthesis is induced for the increased metabolic activity. While recruitment of ADAP is responsible for the increased cell adhesion and formation of the immunological synapse activation of Vav protein leads to actin cytoskeleton reorganization which is necessary for the stable TCR-pMHC interaction (Hwang et al., 2020; Murphy et al., 2017).

1.2.2. Natural Killer Cells

1.2.2.1. Description and Origin. NK cells are important members of the innate immune system. They are responsive to viral infections and tumour growth with their rapid lytic machinery. With their rapid cytokine release of tumour necrosis factor-alpha (TNF-α) and interferon-gamma (IFN-γ), they also act as a bridge between innate immunity and adaptive immunity.(Krzewski & Strominger, 2008). NK cells were first

discovered in mice during the 70s as an unknown type of lymphocyte (Rolf Kiessling et al., 1976) (Herberman Myrthel E Nunn & Lavkin, 1975) however their recognition and killing mechanism remained a mystery until the 80s when Kärre and Ljunggren came up with the missing-self hypothesis. They discovered that NK cells were attacking a lymphoma cell line which is deficient in the MHC class I molecules while the parental MHC class I+ cells were resistant to NK cell cytotoxicity (Karre et al., 1986) (Sivori et al., 2019).

1.2.2.2. Subtypes. NK cells do not express antigen-specific receptors as T cells do and they also lack the expression of the CD3 complex on their surface. Although the expression of CD56 does not directly affect the function of NK cells, the level of its expression is used to divide the NK cells into two functionally distinct subsets. Approximately 90% of the NK cells in the peripheral blood express low levels of CD56 while expressing high levels of Fc-γ receptor III (CD16). The rest 10% lack CD16 expression with a high expression profile of CD56 (Orange & Ballas, 2006). CD56dimCD16+ NK cells are more cytotoxic since they express perforin while CD56brightCD16- ones lack the expression of perforin but they are responsible for the production of cytokines such as IFN-γ when stimulated with IL-12, IL-15 and IL-18. They are considered the regulatory NK cells (Vivier et al., 2008).

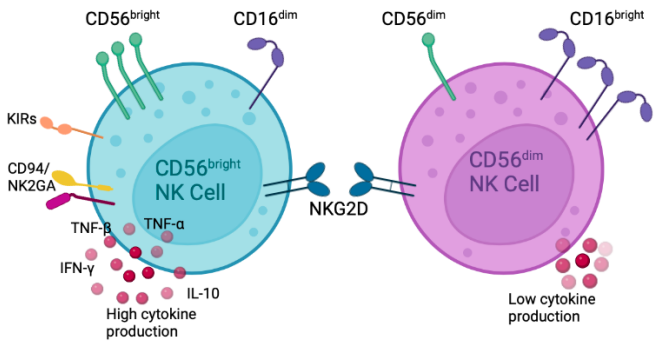

Figure 1.6. NK Cell subsets with different expression patterns of receptors.

Human NK cell subsets also have different expression profiles of NK receptors. While CD56bright NK cells express the killer cell Ig-like receptor (KIR) superfamily at

low levels it is the opposite for the CD56dim subset. On the other hand, a high level of expression of CD94-NKG2A inhibitory receptors is observed in the CD56bright subset while CD56dim have a low expression of these. The activating NKG2D receptor is present in both of the subsets (Figure 1.6.). These different expression profiles of NK receptors result in the different cytotoxicity levels of the NK subsets (M. A. Cooper et al., 2001).

1.2.2.3. Effector Mechanisms. A balance between activating and inhibitory cell surface receptors controls how well NK cells function. Inhibitory receptors carry immunoreceptor tyrosine-based inhibition motifs (ITIMs) in their cytoplasmic tails while activating receptors depend on association with ITAM-bearing adaptor proteins such as CD3ζ, DAP10 and DAP12. There is also another group of activating receptors that interact with non-ITAM bearing proteins.

There are generally two groups of inhibitory receptors which are the immunoglobulin superfamily (KIR, LIR) and the C-type lectin domain family (NKG2A/CD94). When activating receptors recognize their ligands on the target cells, they trigger the activation pathway in NK cells that result in the death of the target cell. On the contrary, inhibitory receptors send negative signals and inhibit the activation pathway when they interact with their ligands on the target cell such as a MHC-I molecules. This interplay between the activating and inhibiting receptors decides whether the NK cell will be activated or not (Krzewski & Strominger, 2008).

Before NK cells are activated there are several steps that need to be accomplished. After contacting the target cell the adhesion of two cells is necessary for the signal transduction. The segregation of the necessary molecules into the contact area and actin cytoskeleton rearrangements are other steps that are triggered by activating receptor engagement and are essential for the function of NK cells. These mechanisms resemble to T cell activation and result in the formation of an immunological synapse (Krzewski & Strominger, 2008). The activating receptors with ITAMs on their cytoplasmic tails initiate the signalling cascade which has many common points with

TCR/CD3 mediated signalling pathway. When activating receptors engage with their ligands, the ITAMs are phosphorylated by Src family kinases such as Lck or Fyn and this recruits Syk and ZAP70 tyrosine kinases and causes their activation. Activation of ZAP70 results in similar signalling cascades in the cell as T cell activation. As a result, an increase in the calcium levels and actin cytoskeleton reorganization lead to the secretion of lytic granules (Paul & Lal, 2017; Vivier et al., 2004).

There are various effector mechanisms in NK cells that can take place after the target recognition and IS formation, varying according to the recognized ligands and utilized receptors. The primary mechanism utilizes lytic molecules such as granzymes and perforin which are stored in cytolytic granules in the NK cell cytoplasm. These molecules are delivered to the target cell upon NK cell activation stimulated when they recognize a foreign MHC on the target cell, or no MHC at all. While perforins form pores on the target cell, granzyme B utilizes these pores to get into the cell and induce apoptosis by activating apoptotic initiator molecules. This is the same way cytotoxic CD8+ T cells act upon target recognition (Abel et al., 2018; Kucuksezer et al., 2021). Another effector mechanism occurs when tumour necrosis factor-related apoptosis-inducing ligand (TRAIL) interacts with a death receptor (DR4 or DR5) on the target cell. This interaction stimulates the DRs and it activates caspase 8 which lead to apoptosis of the target cell. Fas is another receptor that triggers apoptosis on the target cells when it binds to its ligand (Fas ligand(CD95L). Antibody-dependent cellular cytotoxicity (ADCC) is another pathway NK cells employ where they use their Fc receptors to recognise antibodies on the target cells and once activated they release their cytotoxic granules (Murphy et al., 2017; Smyth et al., 2005).

1.2.3. Cellular Immunotherapy of Cancer

Cancer is the second major cause of death in the world and therapy strategies have been developing since the 19th century. Cancer therapy has been limited to methods such as chemotherapy or radiotherapy until the last decade and these methods are mostly unable to discriminate between healthy cells and tumorigenic cells, meaning they are non-specific (Arruebo et al., 2011). Although back in the 1800s William

Coley observed the effect of the immune system on tumour cells when he injected bacterial toxins into cancer patients, the cancer immunotherapy methods developed quite slowly (Dobosz & Dzieciatkowski, 2019). This type of therapeutic approach has emerged recently where our own immune cells are used, modified and/or empowered to fight cancer without harming healthy cells as much as the other cancer therapy types. Cancer immunotherapy uses the advantage of immune cells' cytotoxicity and functions of the immune system in order to overcome the escape strategies that cancer cells develop. There are two branches of cancer immunotherapy, active and passive, categorized according to their ability to boost the host immune response. While active immunotherapies aim to activate the host's immune system, passive immunotherapies involve adoptive transfer of cells or monoclonal antibodies targeting tumours in the patient (Hayes, 2020; Oiseth & Aziz, 2017).

Cellular immunotherapy is a method where live cells are utiliZed and transferred to the patient in order to fight the tumor. It could be also classified as active and passive based on their way of function. Active cellular immunotherapies, such as dendritic cell (DC) vaccines, trigger the host's immune system. On the other hand, passive cellular immunotherapy involves the transfer of cells that already have the ability to target tumour cells, also known as adoptive cellular therapy (ACT) (Armstrong et al., 2001; Hayes, 2020). In the earliest implementations of this type of therapy, autologous lymphocytes that are reactive to tumour cells in the tumour microenvironment (tumour-infiltrating lymphocytes (TILs)) were isolated, expanded ex vivo and then reintroduced into the patient (Figure 1.7.) (Vacchelli et al., 2013).

TILs consist mainly of cytotoxic T cells and helper T cells, with a small subpopulation of NK and B cells (Savas et al., 2016). However, they are not always successful in targeting tumours or it was unfeasible to collect TILs from patients with inaccessible tumours. Furthermore, the T cells in the tumour microenvironment may have already been exhausted at the time they were isolated and thus are unable to proliferate efficiently (Lin & Okada, 2016; Vacchelli et al., 2013).

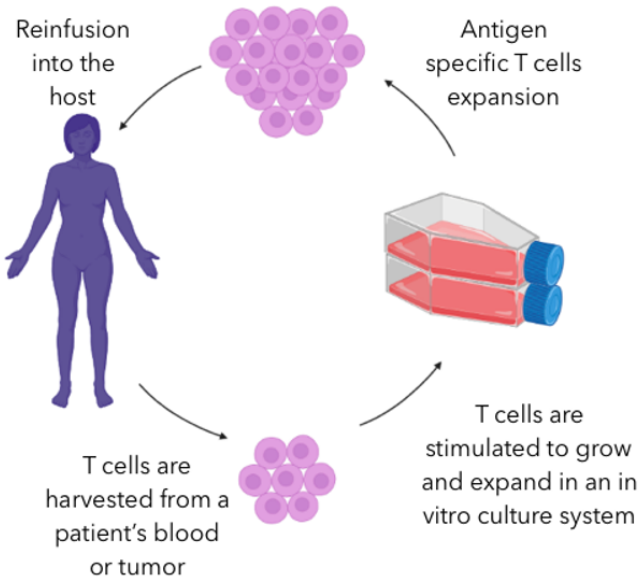

Figure 1.7. Schematic diagram of adoptive cell therapy.

After the identification of T cells from TILs, it was found that these cells can recognize both tumour-specific and tumour-associated antigens (TSA/TAA) with their CD3-TCR complex. While TSAs are expressed specifically on cancer cells TAAs are also expressed in normal cells but have elevated expression patterns on cancer cells (Perica et al., 2015). Since TSAs vary greatly between the patients, TAAs that are shared between most cancer types are commonly utilized in cancer immunotherapy studies. In order to improve the specificity of the ACT method, T cells from TILs that are specific to TAAs were selectively proliferated and given back to the patient. Another groundbreaking method that aims to improve the availability of such treatments is to genetically engineer the T lymphocytes isolated from peripheral blood to target a selected antigen by modifying them with cell surface receptors that are able to recognize TAAs to retarget their specificity. This is performed by either transferring cloned TCR $\alpha\beta$ chain genes idendified from TILs or a synthetic chimeric antigen receptor (CAR) which is specially designed.

1.2.4. TCR-T and CAR-T Cells

While the recognition mechanism of TCR-T cells is restricted to MHCs, CAR-T cells are able to target tumour cells in a non-MHC-dependent manner since the CARs are constructed with an extracellular single-chain antibody variable fragment(scFv) of a monoclonal antibody combined with an intracellular signalling domain and transmembrane domains (Figure 1.8.). Therefore CAR-T cells target extracellular proteins on the surface of tumour cells. However, only about 20% of the proteins produced by the human genome are transmembrane proteins (Lander et al., 2001), thus most of the proteins are out of reach for CAR-T cells which is a disadvantage over TCR-T cells since they are able to target intracellular proteins via MHC complexes.

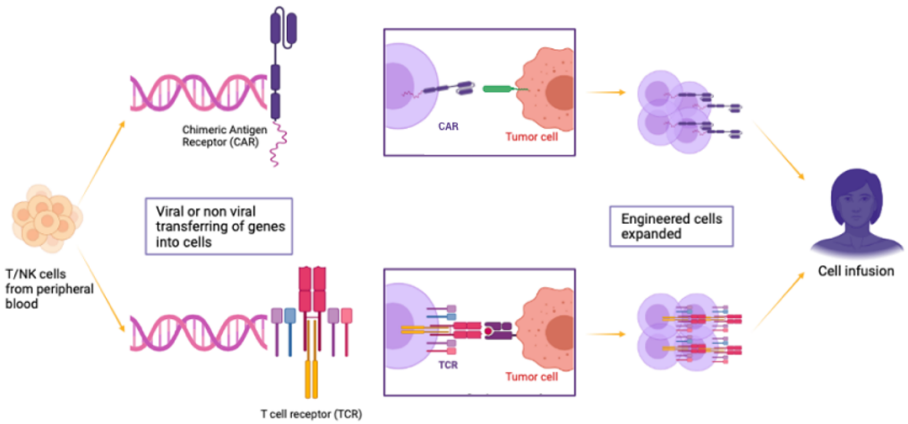

Figure 1.8. Different types of antigen specific immunotherapy.

Melanoma antigen recognized by T cells 1(MART1), tyrosinase and GP100 were the first TAAs identified and used in ACT studies. The TCR alpha-beta chain genes that are reactive against identified TAAs were cloned and used to genetically modify the T cells of cancer patients whose TILs are not effective enough. When T cells are modified with new TCR chains, they become specific to the selected tumour-associated antigen. However, the mispairing problem which is caused by the matching of newly transferred TCR chains and the T cell's endogenous TCR chains is a challenge. If introduced TCR chains match with the complementary TCR chains they produce a TCR complex with unknown specificity and this might cause a problem regarding

autoreactivity and may cause a lethal Graft versus host disease (GvHD) -like syndrome in vivo (Figure 1.9.) (Kershaw et al., 2013; Met et al., 2019).

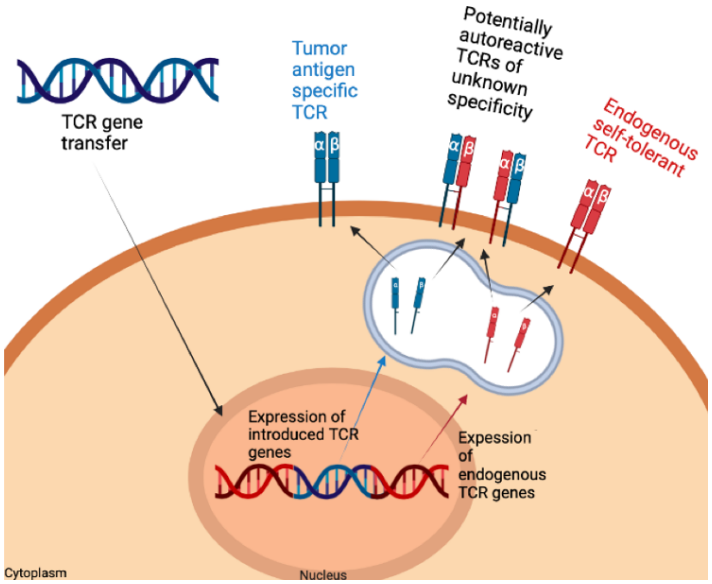

Figure 1.9. Schematic representation of mispairing problem in TCR-T cell immunotherapy.

There has been various studies to overcome the mispairing problem such as utilizing small interfering RNAs in order to downregulate the endogenous TCR chain production (Okamoto et al., 2012), adding extra disulphide bonds between the introduced TCR chains for increasing the chance of correct pairing (Cohen, Li, et al., 2007) or using the constant regins of TCR chains from mice were other trials to prevent mispairing (Cohen, Zhao, et al., 2006) however they have their own risks, too. Therefore the mispairing problem remains a major challenge in TCR-T immunotherapies.

1.2.5. TCR-NK Cells

NK cells first drew attention as tumour-killing lymphocytes in the 70s (Kiessling et al., 1975). They have been used in cancer immunotherapies because of their effective and rapid cytotoxic effects on tumour cells. They kill their targets with a similar mechanism to T cells, by releasing perforin and mediating the granzyme entry pathway (Trapani et al., 2000). Fas ligand (FasL) and tumour necrosis factor-related apoptosis-

inducing ligand (TRAIL) pathways are the alternative methods that NK cells utilise to trigger apoptosis in their target cells. However, cancer cells also developed strategies to escape NK cell cytotoxicity such as decreasing the number of NK cell ligands on their cell surface or expressing specific MHC molecules and KIR ligands to prevent missing-self recognition (Pegram et al., 2009; Wu & Lanier, 2003) . Besides, the tumour microenvironment has limiting effects on the NK cells (Dahlberg et al., 2015). Thus, genetic engineering of NK cells has become a necessity in order to overcome these obstacles.

Modifications can be made to increase the survival and proliferation of NK cells in the tumour microenvironment by upregulating their cytokine secretion such as IL-2, IL-12 and IL-15 (Goding et al., 2007; Tam et al., 1999; Zhang et al., 2004). Although these studies enhance the NK cell cytotoxicity their specificity was limited and can be restricted with MHCs expressed by cancer cells. In order to retarget NK cells, CARs were utilised and since the signalling mechanisms are similar to T cells, promising results have been seen in the clinical trials (Dahlberg et al., 2015; Müller et al., 2020; Wu & Lanier, 2003).

Allogenic and autologous NK cells have been used for CAR-NK studies however there have been limitations in these clinical trials. The isolation and proliferation of NK cells have been an issue since only 5-10% of the PBMCs are NK cells and it takes too much time to get a meaningful number of cells and NK cells isolated from patients are usually suppressed due to the tumour microenvironment. Besides, these blood NK cells have low efficiency of transfection, challenging the transfer of CARs and generating efficient CAR-NK cells. Generation of a stable NK cell line was much needed and several cell lines have been produced throughout the years. None of the NK cell lines has shown such efficiency as the NK92 cell line since it is able to target many cancer types with high and consistent cytotoxicity and is easily transfected. Thus, it is the most common NK cell line that has been used in adoptive cell therapy studies including the production of CAR-NK cells (Dahlberg et al., 2015; Klingemann et al., 2016; Pegram et al., 2009).

However, our group had another plan to utilize NK-92 cells by modifying them with TCR genes to generate TCR-NK cells. Since the endogenous TCR chains are not present in the NK cells the mispairing problem does not exist in this model. Their downstream signalling pathways are similar to T cells, hence NK cells are able to mediate the cytotoxicity triggered upon TCR-pMHC binding. On the other hand, TCR dimers require the CD3 complex for their cell surface expression and signal transduction and NK cells do not have the expression of CD3 subunits except CD3ζ. Thus along with the TCR chain genes, CD3 subunit genes were also required to be delivered to the NK cells. After the successful transfection procedures, our group managed to generate TCR-NK cells with the TCRs being expressed on the cell surface and they observed increased cytotoxicity against A375Tyr cells compared to WT A375 (Parlar et al., 2019). This has been a novel approach for overcoming the mispairing problem in the cancer immunotherapy and was reproduced by other groups both on NK-92 cells and primary NK cells. (Mensali et al., 2019; Morton et al., 2022).

2. AIM

Utilizing TCRs in order to target cancer cells has been a great approach for antigen-specific cancer immunotherapy. However, the mispairing problem was an obstacle in the way for further improving this technique. NK cells were a great option for delivering TCR genes without the risk of mispairing since there are no endogenous TCR chains in them and our group has previously developed TCR expressing NK cells. TCR-NK cells have shown promising results with high cytotoxicity against the cancer cell lines expressing the target antigen of the TCR.

In this study, we wanted to observe if the co-receptor CD8 would have an effect on the cytotoxicity of TCR-NK cells. It has been known that co-receptors mediate TCR-pMHC binding by strengthening the attachment and recruiting Lck to close contact with ITAMs. Although some NK cells express CD8αα homodimer, its role in TCR downstream signalling is not clear and the effect of CD8αβ heterodimer is unknown in TCR-NK cells. We have successfully delivered the CD8 alpha and beta genes to TCR-NK cells and generated three types of cells; TCR-NK-CD8αα, TCR-NK-CD8αβ and TCR-NK-CD8ββ. The cytotoxicity and signalling mechanism of these cells have been evaluated with various assays.

This study aims to;

- Optimize the delivery of lentiviral constructs of CD8 genes to TCR-NK cells,
- Evaluate the effect of CD8 dimers on the cytotoxicity and signalling mechanisms of TCR-NK cells,
- Offer an insight into the distinct functions of CD8 alpha and beta chains in the NK cells.

3. MATERIALS AND METHOD

3.1. Materials

3.1.1. Chemicals

Chemicals that were used in this thesis are listed in the Appendix A section.

3.1.2. Equipments

Equipments that were used in this thesis are listed in the Appendix B section.

3.1.3. Buffers and Solutions

Agarose Gel: 1 g of agarose powder and 100 mL 0.5X TBE buffer were combined for 1% w/v agarose gel and heated to dissolve the agarose. 0.01% (v/v) ethidium bromide was added after the mixture was cooled a little.

Calcium Chloride ($CaCl_2$) Solution: 10 mM PIPES (pH 7.00), 60 mM CaCl2 (from 1M stock) and 15% Glycerol was added together and sterilized via autoclave at 121 °C for 15 minutes. It was stored at 4 °C.

Tris-Borate-EDTA (TBE) Buffer: 54 g Tris-base, 27.5 g boric acid and 20 mL EDTA (pH 8.00) were added together and dissolved in 1 L of ddH2O for 5X stock solution. It was stored at the room temperature and used in 1:10 dilution for 0.5X TBE.

HBS solution (2X): 1.5 mM Na_2HPO_4, 50 mM HEPES and 280 mM NaCl was combined in 250 mL ddH2O. pH was adjusted to 7.1 with 10 M NaOH. It was filtered with 0.22 µm filter and stored at -20°C.b

PEG-8000 50%: 500 grams of PEG-8000 were dissolved in one liter of ddH2O to make one liter of 50% w/v. It was sterilized via autoclave and stored at the room temperature.

Running Buffer (10X): 144.1 g of glycine, 30.3 g of tris-base, and 10 g of SDS were dissolved in 1 liter of ddH2O to make 1 liter of 10X running buffer. It was stored at the room temperature and used in 1:10 dilution for 1X running buffer.

Wet Transfer Buffer (10X): 144.1 g glycine and 30.3 g tris-base was dissolved in 1 liter of ddH2O to make 1 liter of 10X wet transfer buffer. 200 ml of methanol, 100 ml of 10X buffer, and 700 ml of ddH2O were combined to create a 1X working solution and kept at 4°C.

TBS and TBS-T: 88 g NaCl and 24 g tris-base was dissolved in 1 liter of ddH2O to make 1 liter of 10X TBS and pH was adjusted to 7.6. This solution was diluted with ddH2O to a 1:10 concentration to create 1X TBS. To make 1X TBS-T, 1 L of 1X TBS was combined with 1 ml of Tween.

3.1.4. Growth Media

Luria Broth (LB): 20 g LB powder was dissolved in 1 L ddH2O. It was autoclaved at 121 °C for 15 minutes for sterilization. Ampicillin with a final concentration of 100 µg/ml was added to the medium before use for ampicillin selection.

LB-Agar: 16 g LB powder and 12 g bacterial agar powder were dissolved in 800 ml ddH2O for 1X agar medium in 1 L glass bottle. It was autoclaved at 121 °C for 15 minutes for sterilisation. After it was cooled down a little, the appropriate antibiotic was added and it was poured to petri dishes in 10-11 ml. The sterile agar plates were kept at 4 °C after they were solidified.

Complete DMEM: DMEM was used for the maintenance of HEK293FT cell line. 10% heat-inactivated fetal bovine serum, 1 mM Sodium Pyruvate, 0.1 mM MEM Non-

essential amino acid solution, 25 mM HEPES solution and 2 mM L-Glutamine was added to DMEM in a final volume of 500 ml.

RPMI 1640: For the maintenance of NK-92 cell line, 20% heat-inactivated fetal bovine serum, 25 mM HEPES, 1X MEM vitamins, 0.1 mM 2-mercaptoethanol, 1 mM Sodium pyruvate, 0.1 mM MEM Non-essential amino acid solution and 2 mM L-Glutamine was added to RPMI 1640 in a final volume of 500 ml. For the A375, A375Tyr and K562 cell lines, 10% heat-inactivated fetal bovine serum, 1 mM Sodium Pyruvate, 0.1 mM MEM Non-essential amino acid solution, 25 mM HEPES solution and 2 mM L-Glutamine was added to RPMI 1640 in a final volume of 500 ml.

Freezing medium: 6% DMSO (v/v) containing fetal bovine serum (heat inactivated) was used for freezing and storing the cells.

3.1.5. Enzymes

The list of enzymes used in this study are given in Table 3.1.

Table 3.1. List of Enzymes.

Commercial Kit	**Company**
ApaI	New England Biolabs, USA
BamHI-HF	New England Biolabs, USA
CIAP	New England Biolabs, USA
EcoRI-HF	New England Biolabs, USA
MfeI	New England Biolabs, USA
NotI-HF	New England Biolabs, USA
Q5 Polymerase	New England Biolabs, USA
T4 Ligase	New England Biolabs, USA
XhoI	New England Biolabs, USA
XmaI	New England Biolabs, USA

3.1.6. Antibodies

The list of antibodies used in this study are given in Table 3.2.

Table 3.2. List of Antibodies.

Antibody	**Company**
Anti-human CD3 (APC conjugated, clone: SK7)	New England Biolabs, USA
Anti-human CD8 (APC/Cy7 conjugated, clone: SK1)	New England Biolabs, USA
Anti-human CD8 (APC conjugated, clone: RPA-T8)	BD Biosciences, USA
Anti-human CD8β (unconjugated, clone: 5F2)	Santa Cruz Biotechnology, USA
Anti-human CD56 (PE conjugated, clone: 5.1H11)	New England Biolabs, USA
Anti-human CD107a (APC conjugated, clone: H4A3)	New England Biolabs, USA
Anti-human TCR α/β (APC conjugated, clone: IP26)	New England Biolabs, USA
Anti-mouse IgG1 (APC conjugated, clone: RMG1-1)	New England Biolabs, USA
Anti-human TNFα (APC conjugated, clone: MAb 11)	New England Biolabs, USA
Anti-human IFN-γ (APC conjugated, clone: B27)	New England Biolabs, USA

3.1.7. Commercial Kits

The list of commercial kits used in this study are given in Table 3.3.

Table 3.3. List of Commercial kits.

Commercial Kit	Company
Nucleo Spin® Gel and PCR Clean-up Kit	Macheret-Nagel, USA
Nucleo Spin® Plasmid Miniprep Kit	Macheret-Nagel, USA
Nucleo Spin® Plasmid Midiprep Kit	Macheret-Nagel, USA

3.1.8. Bacterial Strains

Escherichia coli (E.coli) Top10 strain is used for general plasmid amplifications and lentiviral construct amplifications.

3.1.9. Mammalian Cell Lines

HEK293FT: A derivation of the human embryonic kidney 293 (HEK293) cell line that produces the large T antigen of the SV40 virus and grows quickly (Invitrogen R70007).

NK92: NK-92 cells are an interleukin-2 (IL-2) dependent natural killer cell line generated from peripheral blood mononuclear cells from a patient with non-Hodgkin's lymphome that is quickly progressing (ATCC® CRL 2407™).

A375: The malignant melanoma cell line A375 originated from a 54-year-old female patient and was isolated in 1973. This cell line is HLA-A2+. (ATCC® CRL-1619™).

A375Tyr: This cell line was constructed from wild type A375 via the transduction of tyrosinase gene. It overexpresses tyrosinase gene.

K562: The first human immortalized myelogenous leukemia line, K562, was derived from a 53-year-old female patient with chronic myelogenous leukemia who was experiencing a blast crisis (ATCC® CCL- 243™).

3.1.10. Plasmids and Oligonucleotides

The list of plasmids and oligonucleotides used in this study are given in Table 3.4. and 3.5.

Table 3.4. List of Plasmids

Plasmid	Purpose	Source
LeGO-iG2puro	Lentiviral construct for GFP expression with IRES.	A kind gift from Prof. Boris Fehse of University Medical Center Hamburg- Eppendorf, Hamburg, Germany
LeGO-iT2puro	Lentiviral construct for tdTomato expression with IRES.	A kind gift from Prof. Boris Fehse of University Medical Center Hamburg- Eppendorf, Hamburg, Germany
LeGO-DGE-IRESpuro	Lentiviral construct for expression of CD3δ, CD3γ and CD3ε with IRES and puromycin resistancy	Lab construct

Table 3.4. List of Plasmids (cont.)

pcDNA3.1-CD8bM-1	Expression plasmid for CD8β gene	Addgene (#40078)
pCI-neo-CD8α	Expression plasmid for CD8α gene	Addgene (#86050)
LeGO-CD8α-iT2puro	Lentiviral construct for expression of CD8α with tdTomato expression and puromycin resistance	Lab Construct
LeGO-CD8β-iT2puro	Lentiviral construct for expression of CD8β with tdTomato expression and puromycin resistance	Lab Construct
pMDLg/pRRE	Virus production/packaging plasmid (Gag/Pol)	Addgene (#12251)
pRSV-REV	Virus production/packaging plasmid (Rev)	Addgene (#12253)
pCMV-VSV-g	Virus production/packaging plasmid (Env)	Addgene (#8454)

Table 3.5. List of Oligonucleotides

Oligo Name	**Purpose**	**Sequence (5' to 3')**
SFFV_Fwd	Confirmation of LeGO-CD8α-iT2-puro and LeGO-CD8β-iT2-puro plasmids.	TGCTTCTCGCTTCTG TTC
IRES_Rev	Confirmation of LeGO-CD8α-iT2-puro and LeGO-CD8β-iT2-puro plasmids.	GCCCTCACATTGCCA AAA
IRES_seqF	Confirmation of LeGO-DGE-IRES-puro plasmid.	TTAAAAAAACGTCT AGGCCC
WPRE_Reverse	Confirmation of LeGO-DGE-IRES-puro plasmids	CATAGCGTAAAAGGA GCAACA
puroR_fwd_ext	PCR for isolation of puromycin resistance gene with forward EcoRI cut site from LeGO.iT2p.	TATTGAATTCTTAT GACCGAGTACAAGCC
puroR_rev_ext	PCR for isolation of puromycin resistance gene with forward XhoI cut site from LeGO.iT2p.	TATACTCGAGCGTAC GATCAGGCGCC

Table 3.5. List of Oligonucleotides (cont.)

CD8b_fwd	PCR for isolation of CD8β gene with forward BamHI cut site from pcDNA3.1-CD8bM-1.	TTATAGGATCCCGCG CCACGATG
CD8b_rev	PCR for isolation of CD8β gene with forward EcoRI cut site from pcDNA3.1-CD8bM-1.	CGCGGATGAATT CTATTCTCTGCT-TATT

3.1.11. DNA Ladder

Appendix C contains the DNA ladder that was utilized in this thesis.

3.1.12. Protein Ladder

Appendix D contains the Protein ladder that was utilized in this thesis.

3.1.13. DNA Sequencing

McLab provided a commercial sequencing service.

3.1.14. Software, Computer-based Programs and Websites

The list of software and websites used in this study are given in Table 3.6.

Table 3.6. List of software and websites.

Software/Websites	Purpose
SnapGene	Constructing vector maps, restriction analysis, DNA sequencing analysis, DNA alignments, etc
Tree Star Inc. Flow Jo	Analyzing flow cytometer data
Addgene Website	Plasmid map and sequence information
GraphPad Software, Inc., San Diego, CA, USA	Data analysis, statistical analysis
Integrated DNA technologies IDT	Designing oligonucleotides
Primer 3 Plus Website	Designing oligonucleotides
Uniprot Website	Human genome sequence information

3.2. Method

3.2.1. Bacterial Cell Culture

Bacterial culture growth: Top10 *E. coli* cells were grown in LB media containing Ampicillin for 16 hours at 37°C with 220 rpm shaking. Glass beads were used to distribute cells over Ampicillin Petri dishes, and they were cultured for 16 hours at 37°C. A single colony was picked from each plate at the end of the incubation period. For glycerol stocks of bacteria, a single colony was cultivated in 3 ml LB media at 37°C with 220 rpm shaking overnight, then diluted 1:3 and cultured at 37°C for 3 hours with

220 rpm shaking at the end of the incubation. Bacteria were harvested during the log phase of development, mixed with glycerol in 1 mL at a final concentration of 10% (w/v), and stored at -80°C in cryotubes.

Preparation of competent bacteria: The glycerol stock of the Top10 *E. coli* cells was used to take a tip of the cells and it was incubated in 3 ml LB without antibiotics at 37°C, with 220 rpm shaking for 4 hours. Then they were transferred into 50 ml LB in a 250 ml flask and incubated overnight at 37°C with 220 rpm shaking. Next day, 4 ml was taken from the culture and transferred to 400 ml LB without antibiotics in a 2L flask. It was incubated at 37°C with 220 rpm shaking until the OD590 reaches around 0.375. After the desired OD is reached, the bacterial culture was split into eight 50 ml-tubes and put on ice for 10 minutes. The tubes were then centrifuged at 1600g for 10 minutes at 4°C. After the supernatants were discarded, 10 ml of ice-cold CaCl2 was added onto the pellets and they were resuspended. They were centrifuged again, this time at 1100g for 5 minutes at 4°C. The supernatants were discarded and 2 ml of ice-cold CaCl2 was added to resuspend the pellets. The tubes were incubated on ice for 30 minutes. The culture was collected in one tube and aliquoted to 1.5 ml tubes in 0.1 ml volume. They were frozen immediately in liquid nitrogen and then stored at -80°C.

Transformation of competent bacteria: The Top10 *E.coli* competent cells and the plasmid DNA were thawed on ice. Plasmid DNA was added to the competent cells and incubated on ice for 30 minutes. After the incubation, the cells were heat-shocked at 42°C for 90 seconds and on ice for 60 seconds. 0.9 ml LB without antibiotics was added to tubes and they were incubated at 37°C with 220 rpm shaking for 45 minutes. Then the cells were centrifuged at 13000 rpm for 1 minute and the 0.9 ml supernatants were discarded. The pellets were resuspended and spread on LB agar petri dishes with the help of glass beads. Plates were incubated at 37°C for about 16 hours.

Plasmid DNA isolation: Plasmid DNAs were isolated by using the manufacturer's protocols of Macherey-Nagel Mini-Midiprep Kits. Concentration and purity measurements of the isolated DNA were made with a NanoDrop spectrophotometer.

3.2.2. Mammalian Cell Culture

Maintenance of cell lines: Complete DMEM with 10% FBS was used for the culture of HEK293FT cells and the cells were maintained in sterile tissue culture flasks with filtered caps at an incubator. The incubation conditions were 37°C with 5% CO2. Cells were split when their confluency was maximum of 90%. The medium was discarded, the cells were washed with PBS and trypsin-EDTA (0.25%) was added to the flasks. The flasks were put in the incubator at 37°C in order to activate the trypsin-EDTA for 5 minutes. After incubation, cells were resuspended in complete DMEM and split with a 1:5 ratio every 2 days.

Complete RPMI 1640 with 20% FBS was used for the culture of NK92 cells with 1000 U/ml human Interleukin-2 (IL2). The cells were maintained in sterile tissue culture flasks with filtered caps at an incubator. The incubation conditions were 37°C with 5% CO2. The cells were usually seeded with 300.000-350.000 cells/ml and IL-2 was added every two days. Complete RPMI 1640 supplemented with 10% FBS without the β-mercaptoethanol was used to maintain T2, K562, A375 and A375Tyr cell lines. The cells were split every two or three days according to their confluencies.

Cell freezing: Suspension cells were set to 500.000 cells/ml density and adherent cells were set to a confluence of 30-40% one day before the freezing. Cells were counted the next day and they were adjusted to be at least 3x106 cells / vial. The cells were then centrifuged at 200g for 5 minutes and the supernatant was discarded. They were resuspended in 0.5 ml FBS for every 3 million cells and incubated for 20 minutes on ice. Meanwhile, FBS with 12% DMSO was prepared and also incubated on ice. After 20 minutes, 0.5 ml FBS with 12% DMSO for every 3 million cells were added to the cells, this way the final concentration of DMSO becomes 6%. The cells were aliquoted in cryotubes in 1 ml volume. They were stored in -80°C for short term and may be transferred to liquid nitrogen for long term storage.

Cell thawing: For every vial to be thawed, 5 ml FBS was placed in 15 ml-tubes. The cryotubes were transferred to room temperature from -80°C or liquid nitrogen.

After the cells were thawed, they are slowly pipetted in the FBS and centrifuged at 200g for 5 minutes. After the supernatant was discarded the pellet was resuspended with the appropriate media, transferred to sterile cell culture flask and placed in the incubator.

3.2.3. Cloning of T Cell Receptors and Co-receptors

3.2.3.1. LeGO.DGE.IRES.puro Cloning. In order to construct LeGO-DGE-IRES - puro vector, forward and reverse primers were designed to extract the puromycin resistance gene from the LeGO-iG2-puro vector. Forward primer has a EcoRI cut site with the sequence of 5'-TAT TGA ATT CTT ATG ACC GAG TAC AAG CC-3' and the reverse primer has an XhoI cut site with the sequence of 5'-TAT ACT CGA GCG TAC GAT CAG GCG CC-3'.

Table 3.7. PCR of puromycin gene from LeGO-iG2puro.

LeGO-iG2p	2.5 ng
NEB 5X Q5 Reaction Buffer	10 µl
10 mM dNTPs	1 µl
10 µM puroR_fwd_ext	2.5 µl
10 µM puroR_rev_ext	2.5 µl
5X Q5 High GC Enhancer	10 µl
NEB Q5 High-Fidelity DNA Polymerase	0.5 µl
ddH2O	Up to 50 µl
Total volume	50 µl

Table 3.8. Condition of PCR for puromycin extraction.

Step	**Temperature**	**Time**
Initial denaturation	98°C	30 seconds
30 Cycles	98°C	10 seconds
	62°C	30 seconds
	72°C	21 seconds
Final Extension	72°C	2 minutes

Following PCR (Table 3.7 and 3.8.), the insert was run on a 0.7% agarose gel prepared with 0.5 TBE at 100 V for 1 hour. Nucleo Spin® Gel and PCR Clean-up Kit were used to clean the gel containing DNA. A NanoDrop spectrophotometer was used to measure the plasmid-containing elution concentration. After that, the insert was cut with XhoI and EcoRI enzymes for 2 hours at 37 °C (Table 3.9.) and it was cleaned up with Nucleo Spin® Gel and PCR Clean-up Kit. The concentration of the final DNA was measured with a NanoDrop spectrophotometer.

The backbone vector LeGO-DGE-IRES-TCR was cut with XhoI and EcoRI enzymes for 2 hours at 37°C (Table 3.10.) in order to remove the TCR region and prepare the vector for ligation of puro gene. Following digestion, the vector was run on a 0.7% agarose gel prepared with 0.5 TBE at 100 V for 1 hour and PCR Clean-up Kit was used to clean the gel containing DNA.

Table 3.9. Digestion of puromycin insert.

PCR product of puromycin	1500 ng
NEB XhoI (10,000 U/ml)	0.75 µl
NEB EcoRI-HF (10,000 U/ml)	0.5 µl
NEB Cut Smart Buffer	5 µl
ddH2O	Up to 50 µl
Total volume	50 µl

Table 3.10. Digestion of LeGO-DGE-IRES-TCR backbone vector.

LeGO-DGE-IRES-TCR	10000 ng
NEB XhoI (10,000 U/ml)	1.5 µl
NEB EcoRI-HF (10,000 U/ml)	1 µl
NEB Cut Smart Buffer	5 µl
ddH2O	Up to 50 µl
Total volume	50 µl

Table 3.11. CIP treatment of the backbone vector.

All LeGO-DGE-IRES-TCR plasmid gel extraction product (except 300 ng which were used for ligation control)	34 µl
NEB CIP (10,000 U/ml)	0.1 µl
NEB Cut Smart Buffer	5 µl
ddH2O	Up to 50 µl
Total volume	50 µl

Following CIP treatment (Table 3.11.), Nucleo Spin® Gel and PCR Clean-up Kit was used to clean the DNA. A NanoDrop spectrophotometer was used to measure the plasmid-containing elution concentration. Ligation was performed according to Table 3.12 for 1 hour at 16°C.

Table 3.12. Ligation reaction of backbone and insert.

Digested puromycin insert	3,5-17 ng
PCR-Clean up product of CIP-LeGO-DGE-IRES-TCR plasmid	50 ng
NEB T4 DNA ligase	1 µl
NEB 10X T4 DNA ligase buffer	2 µl
ddH2O	Up to 20 µl
Total volume	20 µl

Transformation and confirmation of positive colonies: 10 ul from all ligation samples and controls were used to transform 200 µl TopTen competent E.coli cells. After 16 hours at 37°C, colonies were picked to perform colony PCR (Table 3.13 and 3.14.).

Table 3.13. Colony PCR for colonies picked from transformation plates.

10X Taq Buffer	2.5 µl
25 mM MgCl2	1.5 µl
10 mM dNTP	0.5 µl
10 µM IRES-Seqf	0.5 µl
10 µM WPRE rev	0.5 µl
Taq polymerase	0.125 µl
LeGO-DGE-IRES-puro colonies	Colony pick
ddH2O	Up to 25 µl
Total volume	25 µl

Table 3.14. Condition of Colony PCR.

Step	**Temperature**	**Time**
Initial denaturation	95°C	3 minutes
30 Cycles	95°C	30 seconds
	48°C	30 seconds
	72°C	54 seconds
Final Extension	72°C	5 minutes

Following PCR, the samples were run on a 1% agarose gel prepared with 0.5 TBE at 100 V for 1 hour. According to agarose gel image 3 positive colonies were selected and mini cultures were started. 16 hours later, Macherey-Nagel commercial kit was used to isolate plasmid DNAs from mini cultures. Isolated plasmid DNAs were cut with appropriate enzymes in order to confirm the newly constructed plasmid.

3.2.3.2. LeGO-CD8α-iT2p Cloning. pCI.neo.CD8α plasmid were cut with EcoRI and NotI enzymes for 2 hours at 37°C (Table 3.15.) in order to extract the CD8α gene. LeGO.iT2puro vector was cut with the same enzymes for the insert to be cloned in (Table 3.16.).

Table 3.15. Digestion of pCI-neo-CD8α vector.

pCI-neo-CD8α	5000 ng
NEB NotI-HF (10,000 U/ml)	1 µl
NEB EcoRI-HF (10,000 U/ml)	1 µl
NEB Cut Smart Buffer	5 µl
ddH2O	Up to 50 µl
Total volume	50 µl

Table 3.16. Digestion of LeGO-iT2puro vector.

LeGO-iT2puro	10000 ng
NEB NotI-HF (10,000 U/ml)	1 µl
NEB EcoRI-HF (10,000 U/ml)	1 µl
NEB Cut Smart Buffer	5 µl
ddH2O	Up to 50 µl
Total volume	50 µl

Both digested plasmids were run on a 0.7% agarose gel prepared with 0.5 TBE at 100 V for 1 hour. Nucleo Spin® Gel and PCR Clean-up Kit was used to clean the gel containing DNA plasmids. A NanoDrop spectrophotometer was used to measure the plasmid-containing elution concentration.

Table 3.17. CIP treatment of the backbone vector.

All LeGO-iT2p plasmid gel extraction product (except 300 ng which were used for ligation control)	33 µl
NEB CIP (10,000 U/ml)	0.1 µl
NEB Cut Smart Buffer	5 µl
ddH2O	Up to 50 µl
Total volume	50 µl

Following CIP treatment (Table 3.17.), Nucleo Spin® Gel and PCR Clean-up Kit was used to clean the DNA. A NanoDrop spectrophotometer was used to measure the plasmid-containing elution concentration. Ligation was performed according to Table 3.18 for 1 hour at 16°C.

Table 3.18. Ligation reaction of backbone and insert.

CD8α gel extract	4-20 ng
PCR-Clean up product of CIP-LeGO-iT2p plasmid	50 ng
NEB T4 DNA ligase	1 µl
NEB 10X T4 DNA ligase buffer	2 µl
ddH2O	Up to 20 µl
Total volume	20 µl

Transformation and confirmation of positive colonies: 10 ul from all ligation samples and controls were used to transform 200 µl TopTen competent E.coli cells. After 16 hours at 37°C, colonies were picked to perform colony PCR (Table 3.19 and 3.20.).

Table 3.19. Colony PCR for colonies picked from transormation plates.

10X Taq Buffer	2.5 µl
25 mM MgCl2	1.5 µl
10 mM dNTP	0.5 µl
10 µM SFFV_fwd Forward Primer	0.5 µl
10 µM IRES_rev Reverse primer	0.5 µl
Taq polymerase	0.125 µl
LeGO-CD8α-iT2p colonies	Colony pick
ddH2O	Up to 25 µl
Total volume	25 µl

Table 3.20. Condition of Colony PCR.

Step	**Temperature**	**Time**
Initial denaturation	95°C	3 minutes
30 Cycles	95°C	30 seconds
	48°C	30 seconds
	72°C	60 seconds
Final Extension	72°C	5 minutes

Following PCR, the samples were run on a 1% agarose gel prepared with 0.5 TBE at 100 V for 1 hour. According to agarose gel image 3 positive colonies were selected and mini cultures were started. 16 hours later, Macherey-Nagel commercial kit was used to isolate plasmid DNAs from mini cultures. Isolated plasmid DNAs were cut with appropriate enzymes in order to confirm the newly constructed plasmid.

3.2.3.3. LeGO-CD8β-iT2p Cloning. Primers were designed to extract CD8β gene from pcDNA3.1-CD8bM-1 vector purchased from Addgene. Forward primer has a BamHI cut site and a start codon with the sequence of 5'-TTA TAG GAT CCC GCG CCA CGA TG-3'. Reverse primer has a EcoRI cut site with the sequence of 5'-CGC GGA TGA ATT CTA TTC TCT GCT TAT T-3'.

Following PCR (Table 3.21 and 3.22.), the insert was run on a 0.7% agarose gel prepared with 0.5 TBE at 100 V for 1 hour. Nucleo Spin® Gel and PCR Clean-up Kit were used to clean the gel containing DNA. A NanoDrop spectrophotometer was used to measure the plasmid-containing elution concentration.

Table 3.21. PCR for CD8β insert.

pcDNA3.1-CD8bM-1	2.5 ng
NEB 5X Q5 Reaction Buffer	10 µl
10 mM dNTPs	1 µl
10 µM CD8b_fwd Forward Primer	2.5 µl
10 µM CD8b_rev Reverse Primer	2.5 µl
5X Q5 High GC Enhancer	10 µl
NEB Q5 High-Fidelity DNA Polymerase	0.5 µl
ddH2O	Up to 50 µl
Total volume	50 µl

Table 3.22. Condition of PCR.

Step	**Temperature**	**Time**
Initial denaturation	98°C	30 seconds
30 Cycles	98°C	10 seconds
	62°C	30 seconds
	72°C	21 seconds
Final Extension	72°C	2 minutes

Following digestion (Table 3.23.), Nucleo Spin® Gel and PCR Clean-up Kit was used to clean the DNA. A NanoDrop spectrophotometer was used to measure the plasmid-containing elution concentration.

Following digestion (Table 3.24.), the backbone was run on a 0.7% agarose gel prepared with 0.5 TBE at 100 V for 1 hour. Nucleo Spin® Gel and PCR Clean-up Kit was used to clean the gel containing DNA. A NanoDrop spectrophotometer was used to measure the plasmid-containing elution concentration.

Table 3.23. Digestion of CD8β insert.

PCR product of CD8β	500 ng
NEB BamHI (10,000 U/ml)	0.5 µl
NEB EcoRI-HF (10,000 U/ml)	0.5 µl
NEB Cut Smart Buffer	5 µl
ddH2O	Up to 50 µl
Total volume	50 µl

Table 3.24. Digestion of LeGO-iT2p backbone vector.

LeGO-iT2p	10000 ng
NEB BamHI (10,000 U/ml)	1 µl
NEB EcoRI-HF (10,000 U/ml)	1 µl
NEB Cut Smart Buffer	5 µl
ddH2O	Up to 50 µl
Total volume	50 µl

Following CIP treatment (Table 3.25.), Nucleo Spin® Gel and PCR Clean-up Kit was used to clean the DNA. A NanoDrop spectrophotometer was used to measure the plasmid-containing elution concentration. Ligation was performed according to Table 3.26 for 1 hour at 16°C.

Table 3.25. CIP treatment of the backbone vector.

All LeGO-iT2p plasmid gel extraction product (except 300 ng which were used for ligation control)	32 µl
NEB CIP (10,000 U/ml)	0.1 µl
NEB Cut Smart Buffer	5 µl
ddH2O	Up to 50 µl
Total volume	50 µl

Table 3.26. Ligation reaction of backbone and insert.

CD8β gel extract	18 ng
PCR-Clean up product of CIP-LeGO-iT2p plasmid	50 ng
NEB T4 DNA ligase	1 µl
NEB 10X T4 DNA ligase buffer	2 µl
ddH2O	Up to 20 µl
Total volume	20 µl

Transformation and confirmation of positive colonies: 10 ul from all ligation samples and controls were used to transform transform 200 µl TopTen competent E.coli cells. After 16 hours at 37°C, colonies were picked to perform colony PCR.

Following PCR (Table 3.27 and 3.28.), the samples were run on a 1% agarose gel prepared with 0.5 TBE at 100 V for 1 hour. According to agarose gel image 3 positive colonies were selected and mini cultures were started. 16 hours later, Macherey-Nagel commercial kit was used to isolate plasmid DNAs from mini cultures. Isolated plasmid DNAs were digested with appropriate enzymes in order to confirm the newly constructed plasmid.

Table 3.27. Colony PCR for colonies picked from transormation plates.

10X Taq Buffer	2.5 µl
25 mM MgCl2	1.5 µl
10 mM dNTP	0.5 µl
10 µM SFFV_fwd Forward primer	0.5 µl
10 µM IRES_rev Reverse primer	0.5 µl
Taq polymerase	0.125 µl
LeGO-CD8β-iT2p colonies	Colony pick
ddH2O	Up to 25 µl
Total volume	25 µl

Table 3.28. Condition of Colony PCR.

Step	**Temperature**	**Time**
Initial denaturation	95°C	3 minutes
30 Cycles	95°C	30 seconds
	48°C	30 seconds
	72°C	60 seconds
Final Extension	72°C	5 minutes

3.2.4. Production of Lentiviral Vectors

One day prior to the production of VSV-G pseudotyped lentiviral vectors, 4x106 HEK 293FT cells were seeded in 100 mm petri dishes. After 16 hours, cells were transfected with 7.5 µg of vector plasmid (LeGO-DGE-IRES-puro, LeGO-CD8α-iT2p and LeGO-CD8β-iT2p), 3.75 µg pf pMDLg/pRRE, 2.25 µg of pRSV-REV and 1.5 µg of phCMV-VSV-G using calcium phosphate transfection method. Plasmids were mixed with up to 450 µl ddH2O and 2.5 M CaCl2 was added. The plasmid mix was added to 500 µl 2X HBS drop by drop while bubbling the HBS and the mixture was incubated for 15 minutes. In the meantime, 25 µM Chloroquine was added to the medium of the cells that were seeded one day prior. After the incubation, the HBS-plasmid mix

was added to the cells drop by drop while plates were gently moved in a circular motion. After 8 hours the medium was changed with complete DMEM medium. After 48 hours from the medium change, virus-containing supernatant was collected and filtered with 0.45 µm filters and stored in -80°C until further use. By transducing HEK293FT cells with serially diluted volumes of virus supernatant, a small aliquot from each generation was used to evaluate viral titers. If the virus titers are low, in the next virus production, after the collection and filtration of the virus, it is directly PEGylated with a 10% final volume for 16 hours at 4°C. Following the incubation, the virus-PEG mixture was centrifuged at 3000xg for 30 minutes. The supernatant was discarded and the remaining pellet containing viral particles coated with PEG is resuspended in an appropriate amount of serum-free RPMI-1640 medium and stored at -80°C. The viral titers were measured with the same way by transducing HEK293FT cells.

3.2.5. Lentiviral Transduction of NK-92 Cells

NK-92 cells were counted and set to 500.000 cells/ml the day before the transduction. The next day, 1x106 /ml NK-92 cells were seeded in duplicates into T25 tissue culture flasks and mixed with appropriate amount of virus with MOI=5 in the final volume of 6 ml. 8 μg/ml protamine sulfate and 1.5 µM (5Z)-7-Oxozeaenol in a final volume of 6 ml were added to the T25 flasks.

The transduced cells were incubated at 37°C, 5% CO2 for 16 hours. Then the cells were collected and centrifuged at 300xg for 5 minutes at room temperature. After the virus-containing medium was discarded, a fresh medium was added. The cells were kept in the incubator for at least 3 days before gene expression measurements were carried out.

3.2.6. Flow Cytometry

The following protocol was followed for all antibody staining for flow cytometry: For surface staining, the cells were washed once with PBS and incubated with the

appropriate amount of antibody on ice for 30 minutes. Following incubation, stained cells were washed with PBS again and fresh PBS was added for running in the flow cytometry. PE-conjugated CD56 mAb (clone: 5.1H11) was used as a marker for NK cells. For checking TCR/CD3 complex on the surface of NK-TyrTCR-DGE-IRES-puro cells APC-conjugated CD3 (clone: SK7) and APC-conjugated TCR α/β (clone: IP26) antibodies were used. CD8α and CD8β surface expressions were checked with APC-conjugated CD8 (clone: RPA-T8), APC/Cy7-conjugated CD8 (clone: SK1), non-conjugated CD8β (clone: 5F2) and anti-mouse IgG1-APC (clone: RMG-1) antibodies.

For intracellular staining, cells were fixed with a 50% PFA containing 1X wash buffer for 30 minutes. They were washed twice with 1X wash buffer and incubated with the bb appropriate amount of antibody on ice for 30 minutes. Following incubation stained cells were washed twice with wash buffer again and fresh PBS was added for running in the flow cytometry. The data acquisition was performed with the flow cytometer and the data were analysed with the FlowJo software.

3.2.7. Analysis of NK Cell Cytotoxicity by Xcelligence RTCA

xCELLigence real time cell analysis (RTCA) dual purpose (DP) device was utilised to perform a real-time cell viability experiment in an incubator with conditions of 37 °C and 5% CO2. The E16 plates were incubated for 15 minutes with 100 µl of cell-free medium containing 10% FBS. Following incubation, background impedance signal was measured to check all connections of the plates. The target cells, A375 and A375Tyr, were seeded on plates with a concentration of 1x104 and incubated for 30 minutes at room temperature. After that, the plates were placed to the device and incubated for 16 hours. The following day, the effector cells were added to the target cells with the determined ratio (1:1, 0,1:1, 0,3:1). The Cell index (CI) was recorded for 48h by performing real-time measurements every 15 minutes. The RTCA program was used to analyze the data.

3.2.8. Analysis of NK Cell Degranulation

One of the target cells, K562, and effector cells were seeded with a concentration of 5x105 cells/ml one day prior to the experiment. Other target cells, A375 and A375Tyr, were arranged so that they become 80-90% confluent on the experiment day. All cells were counted and set to 2x105 cells in 100 ul per well. The effector NK-92 cells were combined with an appropriate amount of APC conjugated-CD107a antibody at the beginning and they were co-incubated with their target cells for 1 hour at 37 °C at 5% CO2 in a V-bottomed 96-well plate. Ionomycin (final concentration 0.25 µg/ml) and Phorbol 12-myristate 13-acetate (PMA)(Final concentration 1.25 µg/ml) was added to the positive control wells. After 1 hour of incubation, monensin was added to each well with a 1:100 dilution and the plates were further incubated for 3 hours. Following 4 hours of incubation, the plates were centrifuged at 400 g for 5 minutes. The supernatants were discarded and wild-type NK-92 cells were dyed with PE-conjugated anti-CD56 mAb in PBS for 30 minutes on ice. Other wells were resuspended in 0.2 mL PBS and taken to the flow cytometry for acquisition. The wild-type NK-92 cells were washed with PBS and after their supernatants were discarded, PBS was added to them for flow cytometry acquisition. For the time point degranulation, monensin was not utilised in the plates analysed within an hour (15, 30, 45 and 60 minutes). The data were analysed with FlowJo software.

3.2.9. Intracellular TNF-α and IFN-γ Staining

The same protocol was followed as in the degranulation assay except for the addition of CD107a mAb to the cells. Brefeldin A was utilised this time rather than the Monensin. Following the effector-target cells incubation for 4 hours, the plates were centrifuged and their supernatants were discarded. The cells were stained with PE-conjugated anti-CD56 mAb in PBS for 30 minutes on ice. Then the intracellular staining protocol was followed and after the fixation step, the cells were stained with appropriate amounts of APC conjugated-TNF-α and APC conjugated-IFN-γ mAbs. Following the staining, cells were taken to the flow cytometer for data acquisition.

3.2.10. Western Blot Analysis

One of the target cells, K562, and effector cells were seeded with a concentration of 5x105 cells/ml one day prior to the experiment. Other target cells, A375 and A375Tyr, were arranged so that they become 80-90% confluent on the experiment day. The effector cells were counted and set to 2x105 cells in 100 ul per well in complete RPMI medium without the FBS. They were seeded in a V-bottom 96-well plate and incubated for 2 hours in the incubator at 37°C with 5% CO2 for starvation. Following the incubation, target cells were counted and set to 2x105 cells in 100 ul and added to the effector cells. The plate was centrifuged at 50g for 2 minutes. After 1 hour of coincubation in the incubator, cells were collected and lysed with radioimmunoprecipitation assay (RIPA) buffer (200 ul per 1x106 cells) containing protease and phosphatase inhibitors. After 1 hour of lysis at -20 °C, cells were centrifuged and the supernatants were collected. Laemmli buffer was added and the samples were incubated at 95 °C for 15 minutes. Sodium dodecyl sulfate-polyacrylamide gel electrophoresis (SDS-PAGE) was performed with the samples followed by western blotting with PVDF transfer membranes. The membranes were blocked with 5% skim milk for 1 hour after the transfer. Membranes were then incubated with appropriate antibodies for 16 hours at 4°C. The antibodies and their dilutions are as follows: p-PLC γ-1 (Y783), ERK (pan) (cat:51-9001961) and Erk1/2 (PT202/PY204) (cat:51-9001962). The next day, the membranes were washed and incubated with horseradish peroxidase (HRP)-conjugated secondary antibodies appropriate for the primary antibodies' host for 1 hour at room temperature. Then the membranes are visualised using ECL or ECL-Sirius with Syngene G:BOX Chemi Xrq. Quantification was performed on ImageJ.

3.2.11. Statistical Analysis

GraphPad Prism (GraphPad Software Inc. La Jolla, CA, USA, version 9.0.0) was used for the preparation of graphs and statistical analysis. 2-way ANOVA test was utilised to make multiple comparisons.

4. RESULTS

4.1. Cloning of T Cell Receptors and Co-receptors

4.1.1. LeGO.DGE.IRES.puro Cloning

For the puromycin resistance gene cloning into LeGO-DGE-i-TCR (10708 bp) backbone and TCR gene removal, the backbone was digested with EcoRI-HF and XhoI. Puromycin resistance gene (598 bp) was amplified from LeGO-iG2-puro (8503 bp) vector with PCR described in Materials and Methods, and after gel purification, the insert was digested with EcoRI-HF and XhoI enzymes. Ligation was performed as described in Materials and Methods and E. coli cells were used for the transformation of the samples. Colonies were picked to perform colony PCR. Two positive colonies were picked and controlled with digestion. The positive colonies were used for lentiviral vector production.

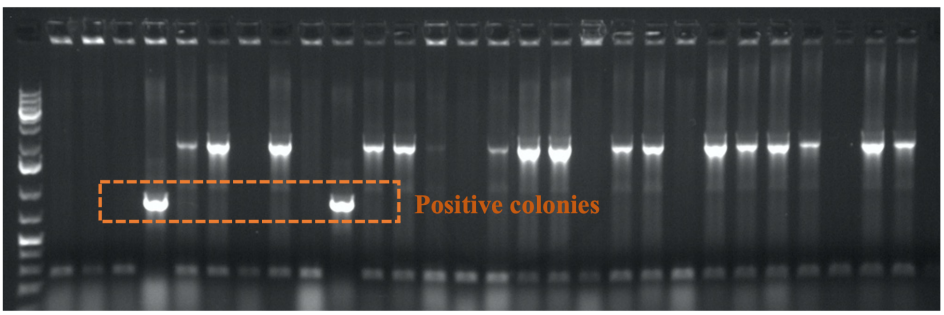

Figure 4.1. Gel image of colony PCR result from LeGO-DGE-IRES-puro colonies.

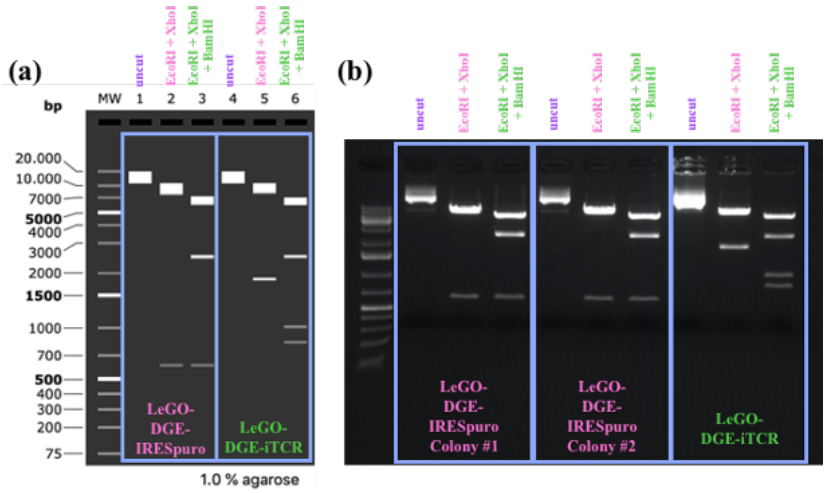

Figure 4.2. Confirmation of LeGO-DGE-IRESpuro cloning with control digestion. A) The gel image of predicted control digestion result. B) The gel image of actual results where both of the colonies were positive.

4.1.2. LeGO.CD8α.iT2p Cloning

For the CD8α cloning into LeGO-iT2p (9214 bp) vector, the backbone was digested with EcoRI-HF and NotI-HF enzymes. The insert (713 bp) was extracted from pCI-neo-CD8α (6175 bp) plasmid with EcoRI-HF and NotI-HF enzymes. Ligation was performed as described in Materials and Methods and E. coli cells were used for the transformation of the samples. Colonies were picked to perform colony PCR. Three positive colonies were picked and controlled with digestion. Confirmed plasmids were used to produce lentiviral vectors.

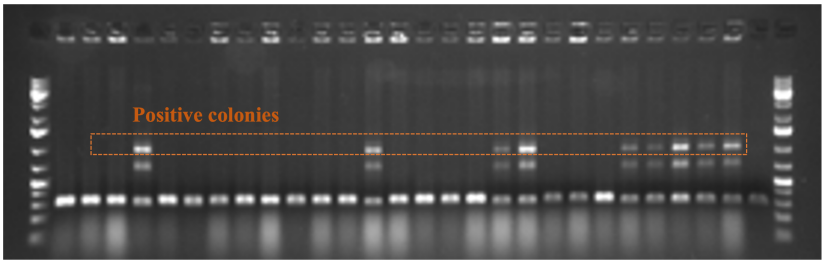

Figure 4.3. Gel image of colony PCR result from LeGO-CD8α-iT2p colonies.

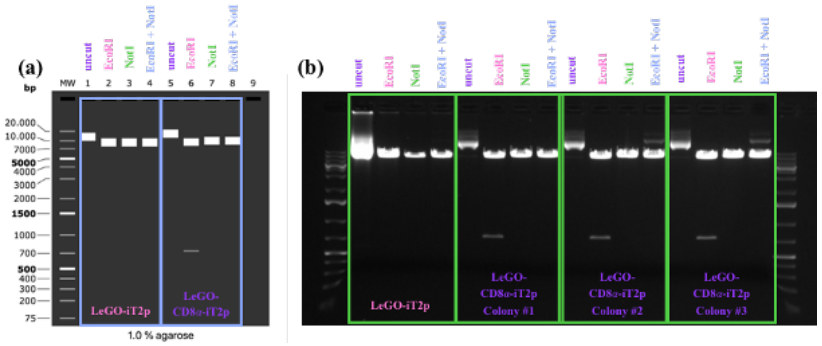

Figure 4.4. Confirmation of LeGO-CD8α-iT2p cloning with control digestion. A) The gel image of predicted control digestion result. B) The gel image of actual results where all of the colonies were positive.

4.1.3. LeGO.CD8β.iT2p Cloning

For the CD8β cloning into LeGO-iT2p (9214 bp) vector, the backbone was digested with BamHI-HF and EcoRI-HF enzymes. CD8β (652 bp) gene was amplified from pcDNA3.1-CD8bM-1 (6052 bp) vector with PCR described in Materials and Methods, and after gel purification, it was digested with BamHI-HF and EcoRI-HF enzymes. Ligation was performed as described in Materials and Methods and E. coli cells were used for the transformation of the samples. Colonies were picked to perform colony PCR. Two positive colonies were picked and controlled with digestion. Confirmed plasmids were used for lentiviral vector production. (Perica et al., 2015)

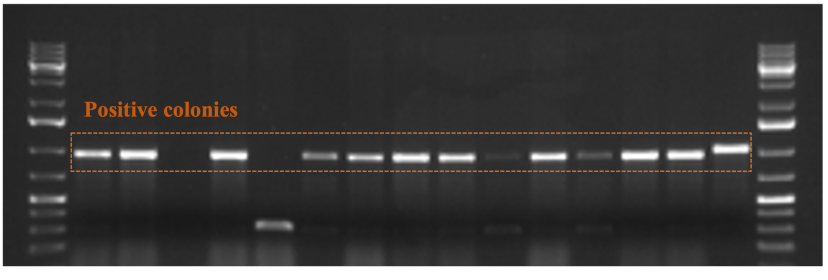

Figure 4.5. Gel image of colony PCR result from LeGO-CD8β-iT2p colonies.

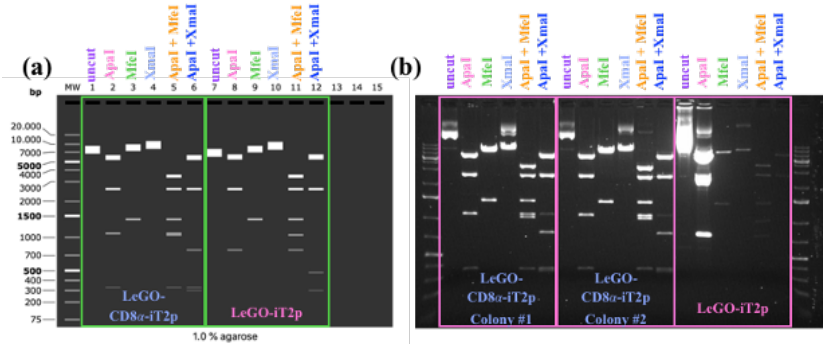

Figure 4.6. Confirmation of LeGO-CD8β-iT2p cloning with control digestion. A) The gel image of the predicted control digestion result. B) The gel image of actual results where both of the colonies were positive.

4.2. Production of Lentiviral Vectors

For the TCR surface expression in NK-TyrTCR cells, CD3 delta, gamma and epsilon chains are necessary. We used a lentiviral vector containing CD3 chain genes (except zeta) and in order to observe the effect of CD8 coreceptor on TCR-NK cells, we constructed 2 lentiviral vectors (Figure 4.7). HEK293FT cells were used for the VSV-G pseudotyped lentivirus production.

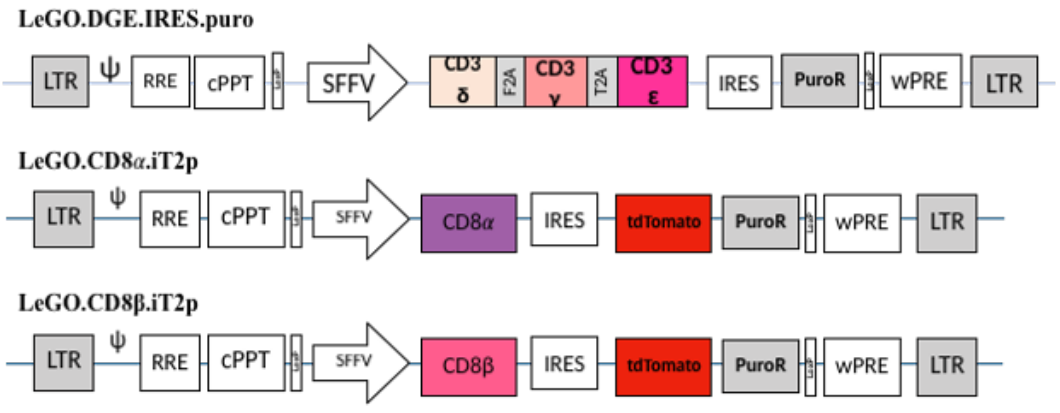

Figure 4.7. Schematic representation of lentiviral constructs used in this study.

Table 4.1. Titration table of lentiviruses.

Lentiviral Vector	**Collection Time**	**Average number of infectious particles x 10^6/ml**
LeGO-DGE-IRESpuro	48h	2,14
LeGO-CD8α-iT2p	48h	2,29
LeGO-CD8β-iT2p	48h	2,09

4.3. Cell Surface Assembly of TCR Complex in NK Cells

4.3.1. Genetic Modification of NK-TyrTCR Cell Line with CD3 Chain Genes

We already had an NK-92 cell line (NK-TyrTCR) modified with TCR genes targetting tyrosinase antigen however it does not have the necessary CD3 subunits. TCR chains and CD3 subunits require each other for their cell surface expression. Since there is only CD3ζ expression in NK cells, other CD3 subunits were delivered to the NK-TyrTCR cell line with LeGO-DGE-IRES-puro construct via the lentiviral transduction method. Following the transduction, puromycin selection was started. Puromycin positive cells were selected in 10 days. The flow cytometry analyses were performed with the surface staining of TCR and CD3 before and after the puromycin selection and the selection was confirmed accordingly.

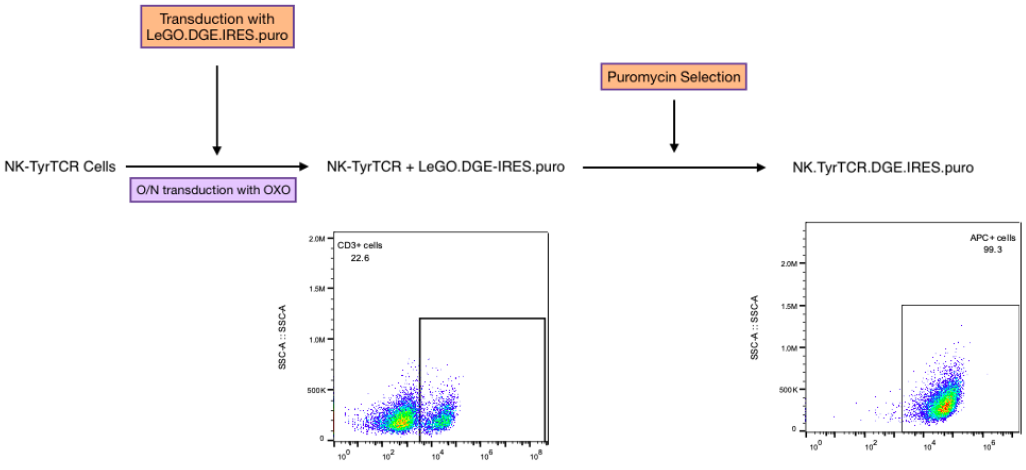

Figure 4.8. Genetic modification process of NK92-TyrTCR cells with LeGO-DGE-IRES-puro lentiviral vector and sorting with puromycin selection results on flow cytometry showing CD3 expression.

4.3.2. Genetic Modification of NK-TyrTCR-DGEip Cell Line with Coreceptor Genes

After the TCR-CD3 complex was succesfully expressed on the surface of the NK92 cells, CD8 alpha and beta chain genes were delivered to these cells with the lentiviral transduction method. LeGO-CD8α-iT2p and LeGO-CD8β-iT2p lentiviruses were used to generate NK-TyrTCR-DGE-IRES-puro-CD8α, NK-TyrTCR-DGE-IRES-puro-CD8β and NK-TyrTCR-DGE-IRES-puro-CD8αβ cell lines. After 1 week following the transduction, transduced cells were surface stained to observe the expression of CD8 coreceptors. Then the cells were sorted by FACS. Following FACS, another surface staining was performed and more than 90% of the cells were observed to express transduced CD8 genes.

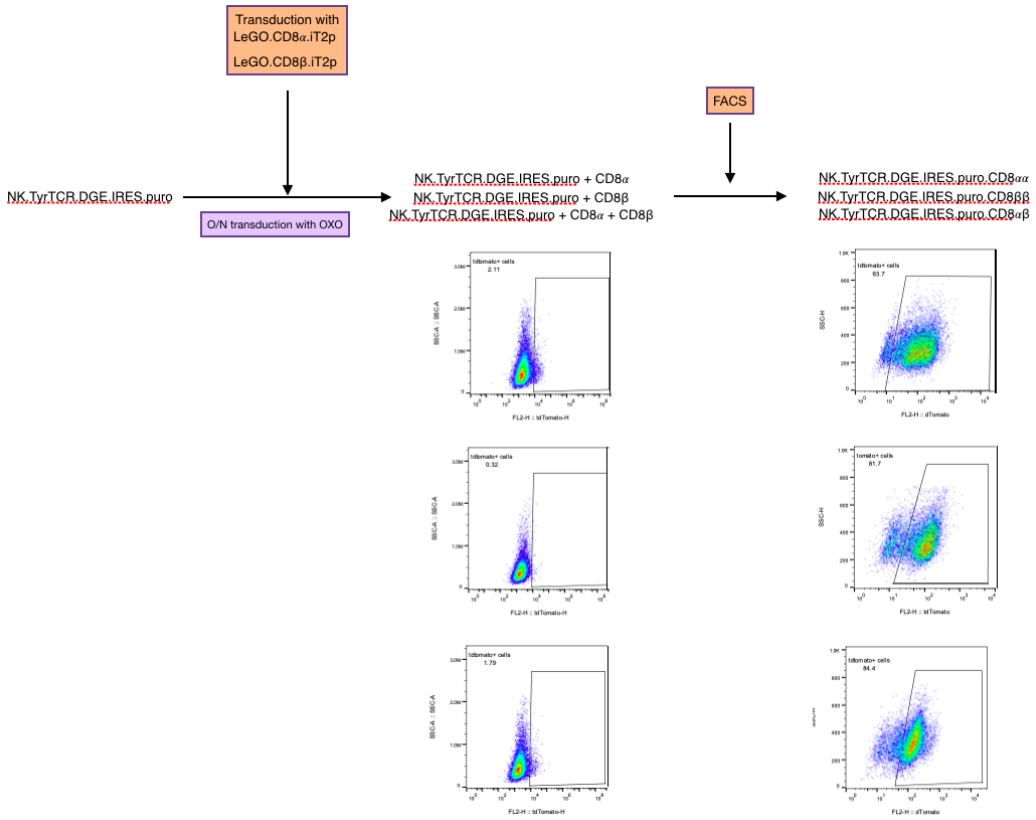

Figure 4.9. Genetic modification process of NK92-TyrTCR-DGE-IRES-puro cells with CD8 lentiviral vectors and FACS sorting results on flow cytometry.

Genetic modification and sorting processes were successful as the CD3 and td-Tomato expression levels show in the Table 4.2. Since the cells with CD8 expression are ready, the functional assays were performed as the next step.

Table 4.2. Results of the lentiviral transductions and selection/sorting

Cell Name	**MOI**	**Transduction Results**	**After Selection or Sorting**
NK-TyrTCR-DGE-IRES-puro	5	22,6%	99,3% (CD3)
LeGO-CD8α-iT2p	5	2,11%	93,7% (tdtomato)
LeGO-CD8β-iT2p	5	0,32%	81,7% (tdtomato)
LeGO-CD8αβ-iT2p	5	1,79%	84,4% (tdtomato)

4.4. Triggering and Specificity of CD8-expressing TCR-NK Cells

4.4.1. Degranulation of CD8-expressing TCR-NK Cells

K562, A375 and A375Tyr cell lines were utilized to investigate the functionality of CD8-delivered NK-TyrTCR-DGE-IRES-puro cells. The levels of CD107a were measured in flow cytometry in order to measure the cytotoxicity. The ratio of effectors/target cells (E/T) was 1:1.

We first performed a standard degranulation assay where the target and effector cells are coincubated for 4 hours. As seen in figure 4.10., we observed that CD8α, CD8β and CD8αβ modifications increased degranulation against K562 and A375. We also observed CD8α, CD8β and CD8αβ modifications increase antigen-specific degranulation against A375Tyr but the extent of this increase was very modest since the original TCR-NK cells already respond at a high level.

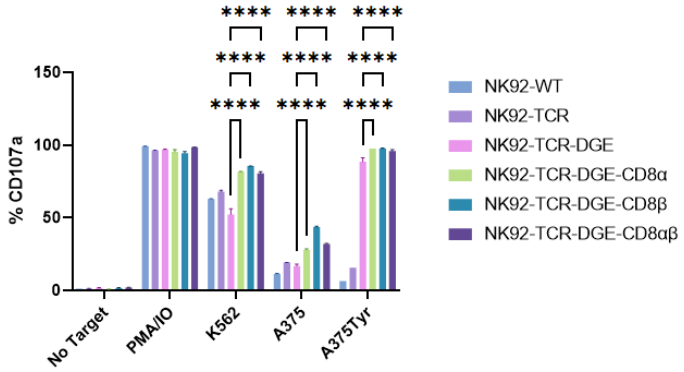

Figure 4.10. Degranulation of NK92-TCR-DGE-CD8 cells.

In order to see triggering dynamics, we performed a time point degranulation assay where we measure the CD107a levels at earlier time points starting at 15 minutes. We observed faster degranulation dynamics in CD8αβ and CD8β cells while CD8α cells responded slower. Nevertheless, all cells reached their full potential within 4 hours (Figure 4.11.).

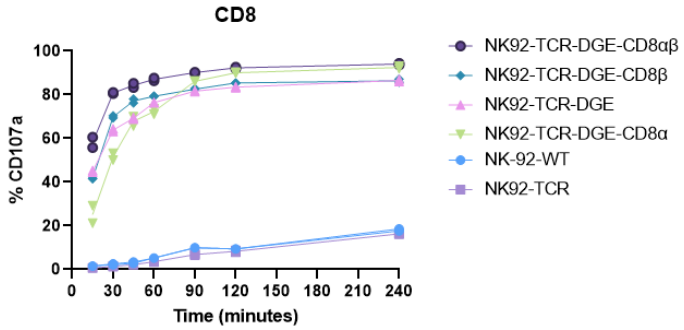

Figure 4.11. Degranulation of NK92-TCR-DGE-CD8 cells at different time points.

4.4.2. Cytotoxic Activity of CD8-expressing TCR-NK Cells

In order to observe the cytotoxicity of our TCR-NK cells, adherent target cells, A375 and A375Tyr, were seeded to E16 plates of xCelligence machine and after 16h of incubation, effector cells were added. Cell index is measured by golden electrodes at the well's surface and reflects overall cell number, adhesion quality, and cell morphology,

which can tell about the growth of tumour cells. This gives us information about the cytotoxic activity of different NK cell lines against antigen-positive and negative targets. We are able to observe a consistent antigen-specific response against A375Tyr cell line while there are different responses to A375 cell line. We first performed the assay with the 1:1 ratio of effector/target cells.

Although we have seen some significant differences within the first 2 hours we wanted to further observe the detailed differences when CD8 genes are present in our cells. For this purpose we have repeated the assay with effector:target ratio of 0.1:1 with the same conditions but could not observe any important difference between the effector cells (Figure 4.14. and Figure 4.15.).

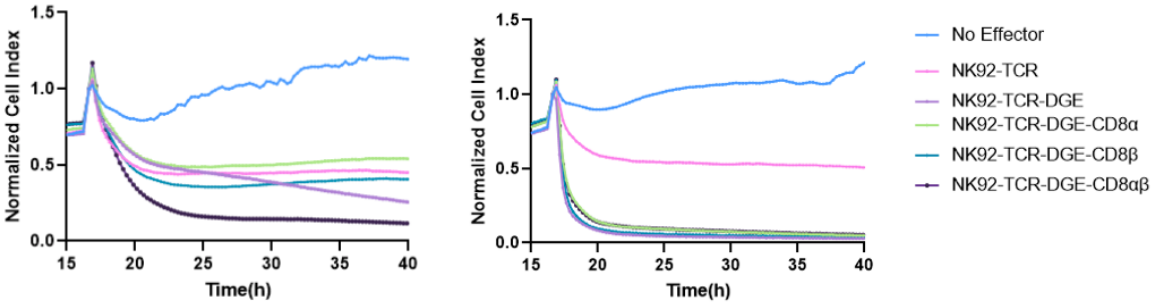

Figure 4.12. Real-time cell analysis of different effector cells against A375 and A375Tyr cells.

Following the effector addition at 16 hours, cell index was measured by the equipment with 15 minutes intervals for 40 hours. Cell index normalized to 1 at the time of effector cell addition. E:T = 0.1:1.

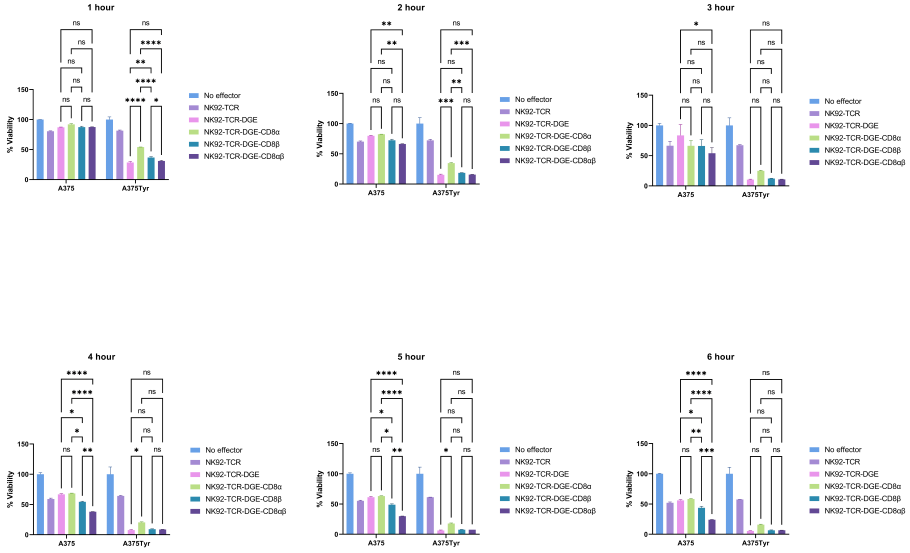

Figure 4.13. Cell index measurements at different time points which were baseline-corrected to no effector cell indexes. E:T = 1:1.

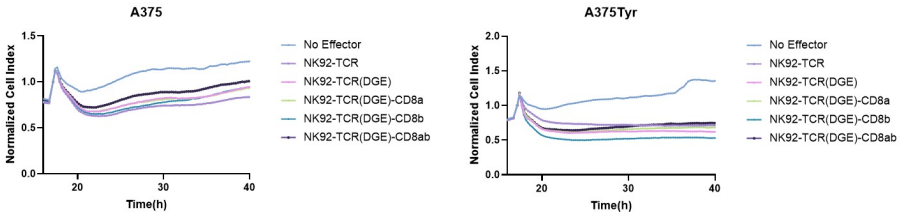

Figure 4.14. Real-time cell analysis of different effector cells against A375 and A375Tyr cells. E:T = 0.1:1.

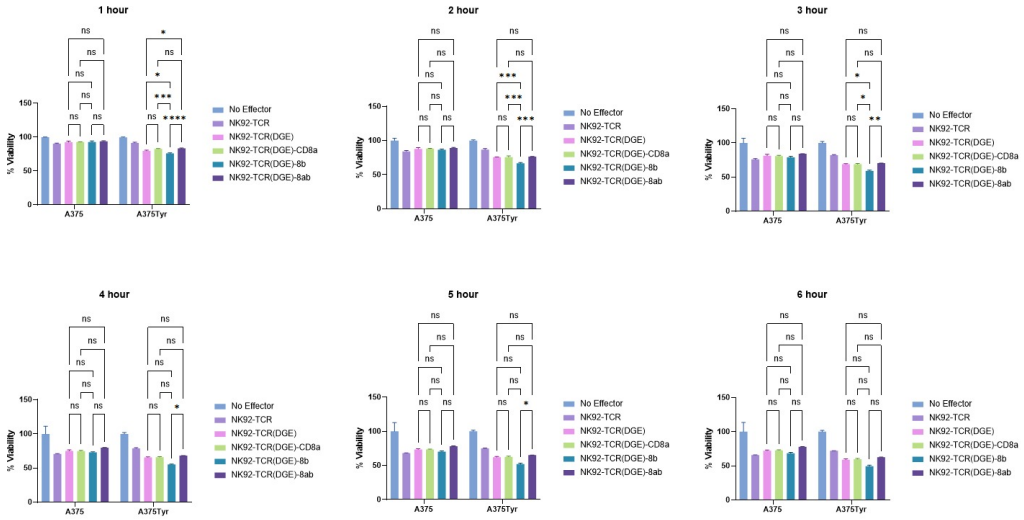

Figure 4.15. Cell index measurements at different time points which were baseline-corrected to no effector cell indexes. E:T = 0.1:1.

We then increased the effector number to see a difference however could not observe any significant difference this time, either. The effector:target ratio was 0.3:1. (Figure 4.16. and Figure 4.17.)

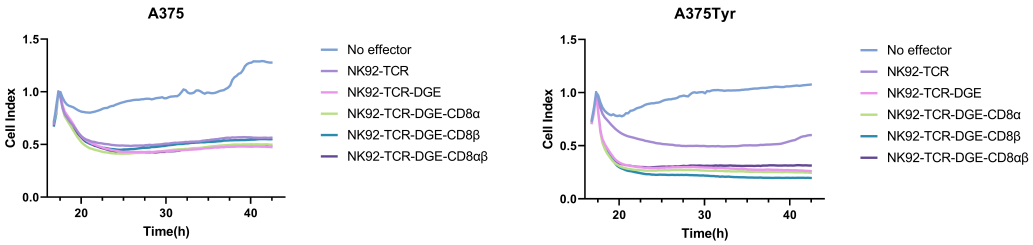

Figure 4.16. Real-time cell analysis of different effector cells against A375 and A375Tyr cells. E:T = 0.3:1.

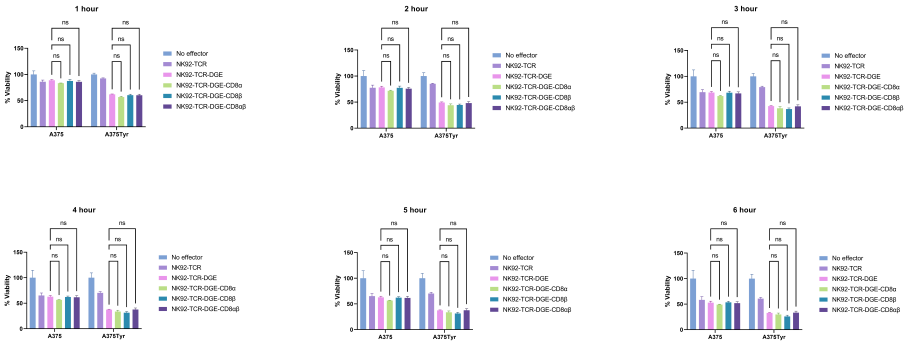

Figure 4.17. Cell index measurements at different time points which were baseline-corrected to no effector cell indexes. E:T = 0.3:1.

4.4.3. TNF-α and IFN-γ secretion of CD8-expressing TCR-NK Cells

Activated NK cells secrete cytokines including TNF-α and IFN-γ and we wanted to measure the levels of these cytokines with a flow cytometry-based assay. After the coincubation of effector and target cells with a ratio of 1:1 for 4 hours, they were intracellularly stained with TNF- α and IFN-γ antibodies.

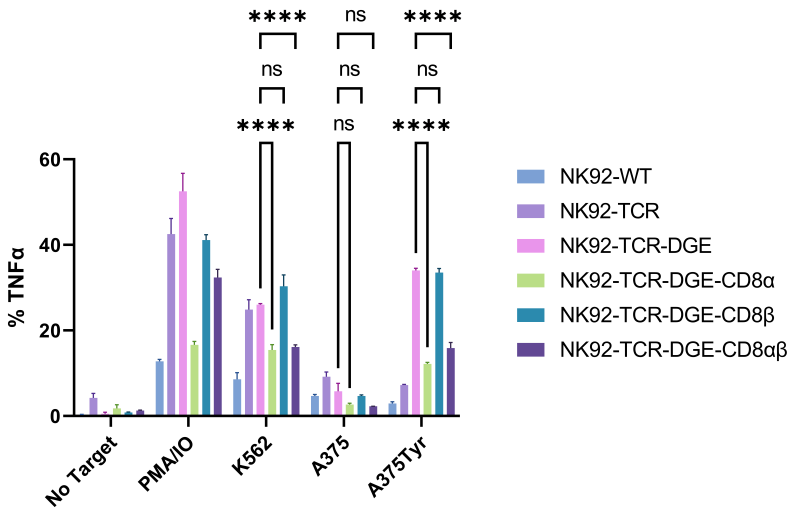

Figure 4.18. TNFα secretion levels of stimulated TCR-NK cells represented with a bar graph.

We observed decreased TNFα levels in TCR-NK cells expressing CD8α either alone or in combination with CD8β against K562 and A375Tyr target cells while the TCR-NKs that only express CD8β have a similar TNFα expression level as regular TCR-NK cells. There were no significant differences between the TNFα levels of effector cells when stimulated with A375 cells (Figure 4.18 and Figure 4.20.).

The flow cytometry analyses of IFNγ cytokine levels show a similar pattern as TNFα levels. Effector cells containing CD8α gene either alone or in combination with CD8β released less cytokine than the NK92-TCR-DGE and NK92-TCR-DGE-CD8β cells when stimulated with K562 or A375Tyr. A375 stimulation results in different IFNγ expression levels for the effector cells containing CD8β gene which is higher. (Figure 4.19. and Figure 4.21.).

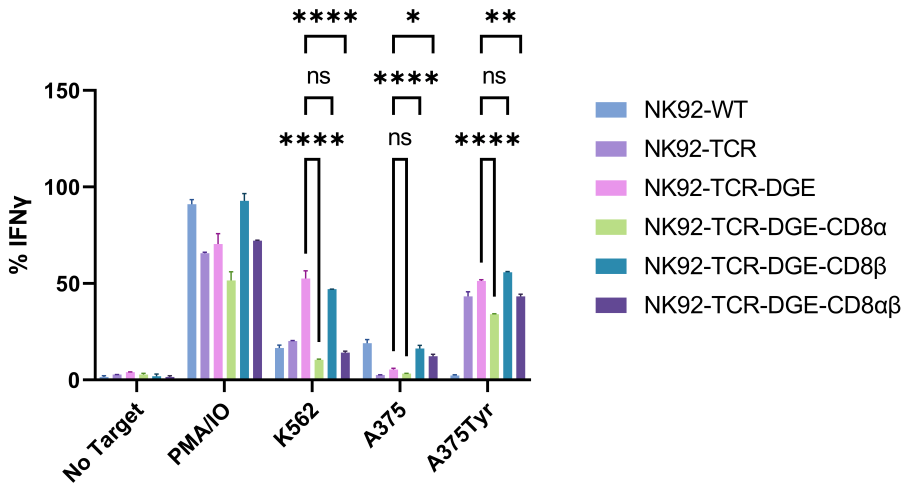

Figure 4.19. IFNγ secretion levels of stimulated TCR-NK cells represented with a bar graph.

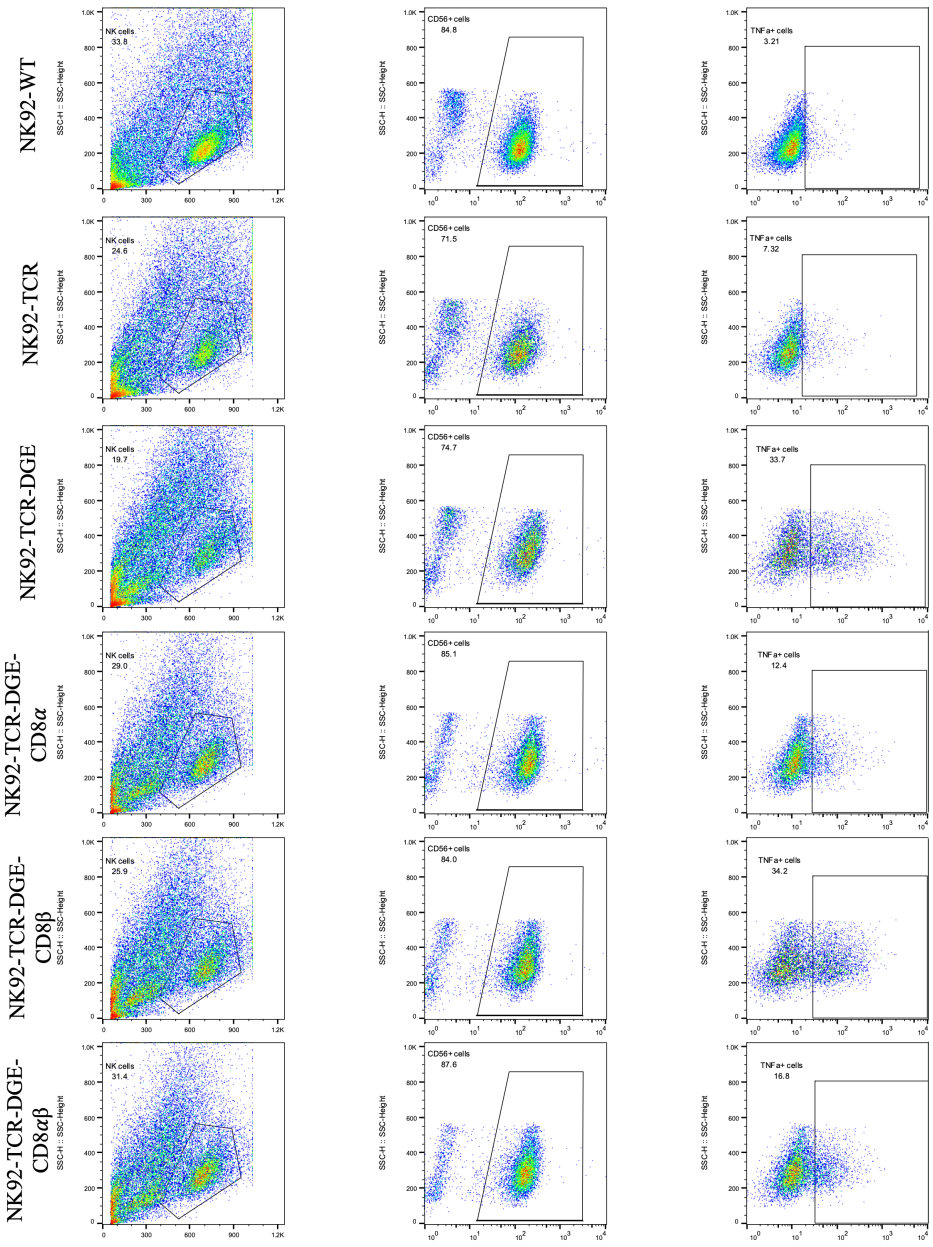

Figure 4.20. Flow cytometry analysis of TNFα secretion levels released by effector cells against A375Tyr cells.

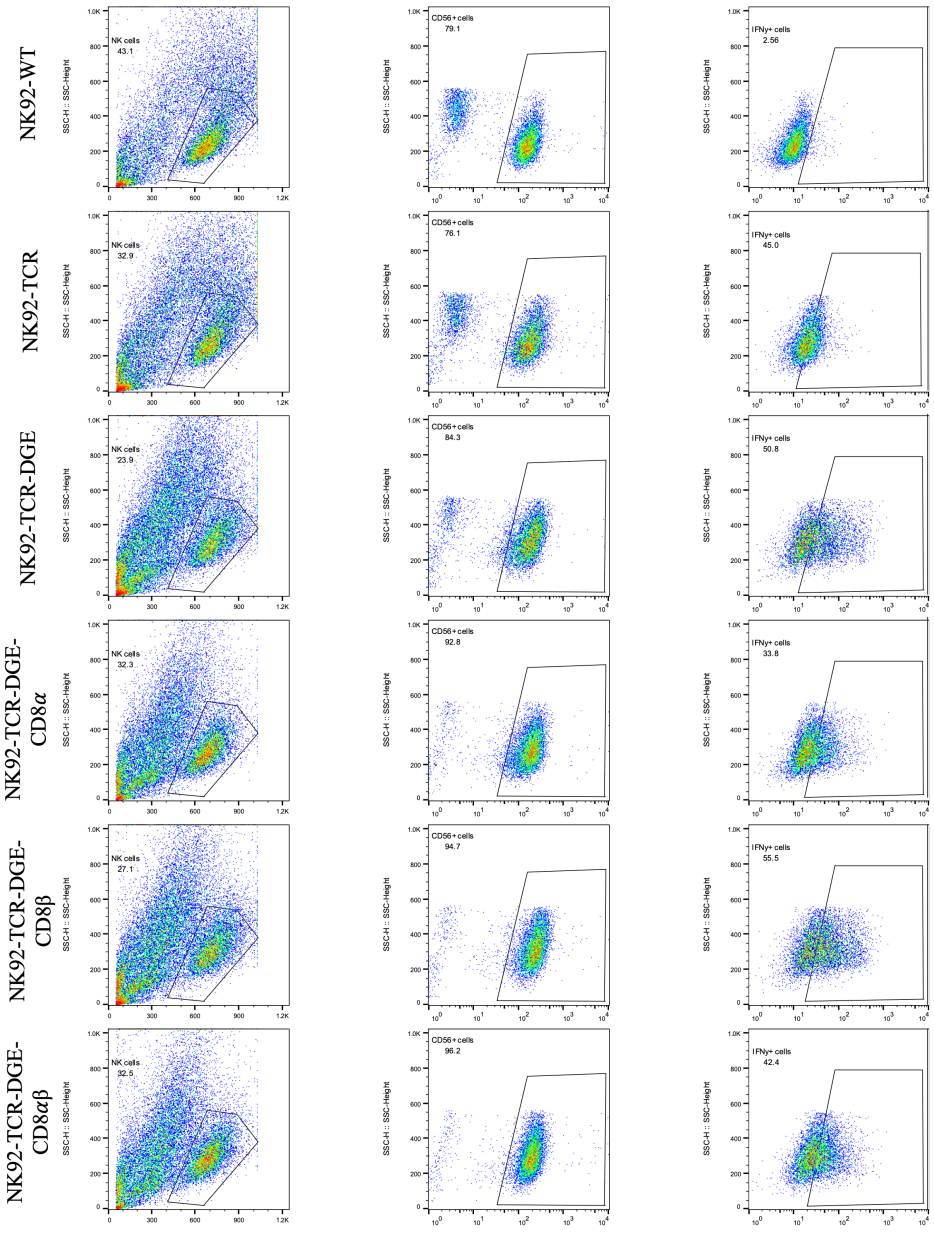

Figure 4.21. Flow cytometry analysis of IFNγ secretion levels released by effector cells against A375Tyr cells.

These cytokine secretion assay results indicate that there might be a way that CD8α receptors affect the secretion of cytokines, TNFα and IFNγ, in a negative way while CD8β receptors only have an effect for IFNγ levels when stimulated with A375 cells.

4.4.4. Protein Analysis of CD8-expressing TCR-NK Cells

There are various proteins phosphorylated in the downstream signalling pathway of TCR transduction. We wanted to observe the phosphorylation patterns of our effector cells by performing western blot analysis. After the co-incubation of effector cells with target cells under serum starving conditions, PLCγ1 and Erk1/2 proteins were investigated whether they have different phosphorylation levels in our CD8 treated effector cells once these cells are activated.

We observed that CD8α, CD8β and CD8αβ modifications increase PLCγ1 phosphorylation against K562 but do not have such an effect against the non-specific A375 cells. The specific response against A375Tyr presents with the highest level of PLC phosphorylation when CD8α and CD8β are both present (Figure 4.22.).

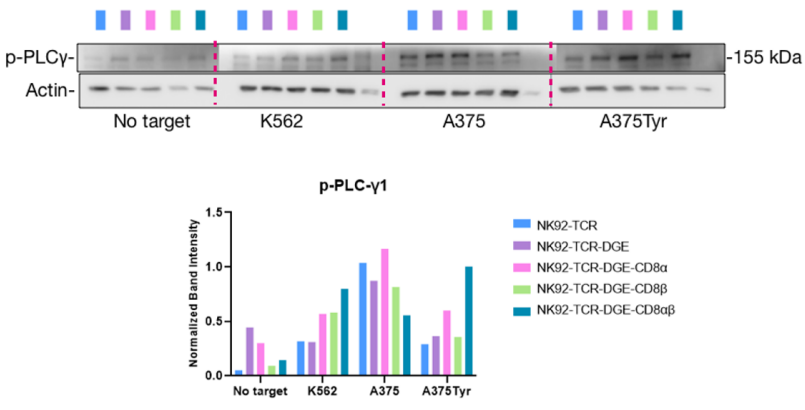

Figure 4.22. Phospho-PLCγ1 expression levels of effector cells stimulated with target cells for 1 hour.

Our analysis of phospho ERk1/2 also confirms previous observations and furthermore shows no increased non-specific activity against K562 or A375. We have seen that

expression of either CD8 chain slightly increases Erk1/2 phosphorylation and the co-expression of both chains dramatically increases response (Figure 4.23.). These results confirm our previous observations that signaling dynamics are faster with a full CD8αβ complex accompanying the antigen-specific TCR.

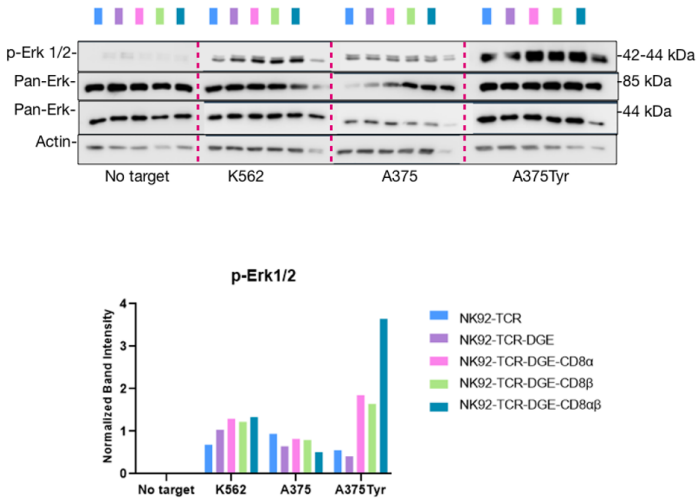

Figure 4.23. Phospho-Erk1/2 and total Erk expression levels of effector cells stimulated with target cells for 1 hour.

5. DISCUSSION

Adoptive immunotherapy has shown great development since it has been first discovered in1980s. It is becoming faster and more specific with the developing technology and genetic engineering methods. Although the first attempts were not unsuccessful, antigen-specific methods increased the efficiency of targeting the tumour cells. While the first clinical trials utilised T lymphocytes harvested from cancer patients without any contextual changes, genetic modifications are now applied to target tumour cells specifically (Vacchelli et al., 2013). There are two common ways to achieve this, chimeric antigen receptors (CARs) and T cell receptors. While TCR-T cells are restricted to peptides presented on MHCs, CAR-T cells can target any surface protein without the need of MHC. However, CAR-T cells have another limitation where they can only target surface protein while TCR-T cells are able to recognise intracellular protein via MHC. Since approximately 75% of the proteins are intracellular, this gives TCR-T cells an advantage over CAR-T cells. On the other hand, the mispairing problem has been a major problem for TCR-T cells. The risk of pairing between exogenous and endogenous TCR chains results in T cells with unknown specificity. Although there have been several studies to overcome this problem it remains unsolved (Restifo et al., 2012).

In the 1970s, NK cells gained attention as lymphocytes that may eradicate tumours. Due to their fast and efficient cytotoxic effects on tumour cells, NK cells have been employed in cancer immunotherapies. Similar to T cells, they destroy their targets by secreting perforin and facilitating the granzyme entry pathway (Trapani et al., 2000). Therefore, these cells were great replacements for T cells since they have all the necessary downstream signalling molecules that are employed in TCR signalling. Moreover, NK cells do not have any endogenous TCR chains which offer a solution for the mispairing problem (Pegram et al., 2009). Our group has previously developed and produced TCR-NK cells and showed successful cytotoxic effects against their target cells A375Tyr (Parlar et al., 2019).

The first step of this study was to clone the CD3 subunits into a lentiviral vector. Since we already have NK92 cells expressing TCR chains that recognise tyrosinase ligand, we needed to add CD3 chains to these cells with lentiviral transduction for TCR expression on the surface. After we successfully generated NK92-Tyr-TCR-DGE cells it was time to add CD8 genes which were cloned to the LeGO-iT2p vector. CD8α and CD8β lentiviruses were used to transduce the cells together and also alone to construct CD8αα, CD8ββ and CD8αβ dimers. To boost the transduction of NK92 cells by blocking the intracellular antiviral defence mechanism, all transductions were conducted in the presence of the TAK1 inhibitor (5Z)-7-Oxozeaenol.

After we successfully sorted our TCR-NK cells expressing CD8 genes with FACS, these effector cells were ready to be analysed with functional assays. Degranulation was the first one we performed and it showed that the presence of both CD8 alpha and beta genes (together or alone) increased the degranulation levels of TCR-NK cells against K562, A375 and A375Tyr. While the response against K562 and A375 was non-specific and does not relate to the CD8 binding to the MHC, it might be caused by the Lck recruitment by the CD8 chains (Mørch et al., 2020). The increased response against A375Tyr was minimal compared to TCR-NK cells that already respond at high levels.

In order to observe the earlier degranulation dynamics in our effector cells, we measured the CD107a levels at earlier time points such as 15, 30, 45 and 60 minutes. We observed that the TCR-NK cells expressing only CD8α showed a slower degranulation compared to CD8β and CD8αβ cells while these two cells showed a higher degranulation compared to TCR-NK cells. It has been reported that CD8αα homodimer has shown co-suppressor effects in T cells by disrupting the lipid rafts and pulling away the signalling molecules away from the immunological synapse (Cheroutre & Lambolez, 2008). The reason why TCR-NK-CD8α cells showed slower degranulation might be this behaviour of the CD8αα homodimer. It was surprising to see that CD8ββ homodimer expressing cells degranulate similarly with the CD8αβ expressing TCR-NK cells since CD8ββ homodimerization does not normally occur in T cells. CD8β normally requires CD8α to move up to the cell surface, however, it has been observed that it is possible

to form a homodimer and function at the cell surface for CD8β in the absence of CD8α. (Devine et al., 2000) Even though the binding capacity of CD8ββ to MHC-I is very low, it might be affecting the NK cell degranulation in other aspects such as Lck recruitment, lipid raft formation or other unknown yet-to-be-explored NK cell signalling dynamics.

Functional assays were followed up by RTCA in xCelligence where cell index measurements were taken to observe the cytotoxicity of our effector cells expressing CD8 genes. TCR-NK cells with CD8αα showed less cytotoxicity against A375Tyr cells compared to other CD8-modified cells and further confirmed our degranulation results. The responses against A375 cells also differ between the effector cells where TCR-NK-CD8αβ showed the highest cytotoxic effect among the other effector cells after 4 hours of coincubation. While the cytotoxicity differences between effector cells against A375Tyr decrease as the co-incubation time increases, it is quite the opposite for the response to A375 cells. This might be caused by the early specific response depending on the addition of co-receptors which interact with the peptide-MHC complex. While on the other hand, the non-specific response is increased when the interaction takes place and the downstream signalling cascade begins where coreceptors might have an effect on the cytoplasmic area by their ability to recruit Lck and other signalling molecules (Gascoigne et al., 2010; Mørch et al., 2020).

Since the antigen-specific response was really fast and reached its full potential within 6 hours, we wanted to repeat this assay with a lower effector:target ratio which was 0.1:1. This time we could not see any important significant difference between the effector cells thus we conducted another assay where the effector:target ratio was 0.3:1. However there was not any significant difference, either.

Cytokine secretion profile of the effector cells was analysed with flow cytometry after the effector cells and target cells were coincubated for 4 hours. Intracellular stainings for TNFα and IFNγ were performed and the results indicate that in the presence of CD8α gene, both cytokine levels were decreased compared to NK-92-TCR-DGE and NK92-TCR-DGE-CD8β cells. This response was present when cells were

stimulated with K562 or A375Tyr cells. Cytokine secretion levels were different when the effector cells were triggered with A375 cells. While there was not any significant difference for the TNFα expression levels, IFNγ levels were higher for the effector cells containing CD8β genes. It can be indicated that the CD8α chain negatively affects the cytokine secretion for the antigen-specific response. However, the non-specific response for the K562 cells was also affected in the same way while A375 response was not affected. This prevents us to reason these changes and requires further investigation.

The decrease might be explained by the co-suppressor features of CD8αα homodimer as aforementioned. It has been demonstrated that this homodimer might be disrupting the lipid raft formation and thus affecting the activation through TCR-CD3 and decreasing the cytokine secretion levels (Cheroutre & Lambolez, 2008). However, it is puzzling to see a decrease in the response of effector cells containing CD8αβ heterodimer since it is the co-receptor that cytotoxic T cells utilise and it is known that these cells also secrete TNFα and IFNγ (Freeman et al., 2012). It is also interesting to see increased IFNγ expression levels when the effector cells containing CD8β chains were stimulated with A375. Perhaps these complicated and unconnected outcomes are the result of various activated signalling pathways in NK cells when they are triggered via TCR-CD3 complex in the presence of CD8 co-receptors.

In order to investigate the downstream signalling pathway alterations, we performed western blot assays on effector cells that are activated by target cells. The phosphorylation profiles of PLCγ1 and Erk1/2 were analysed and the results were consistent with our earlier findings. The highest phosphorylation levels belong to the NK-TCR-CD8αβ effector cell activated by A375Tyr which shows the antigen-specific response. PLCγ1 phosphorylation against K562 was slightly higher when the CD8 genes are present which is not directly linked to CD8 genes since it is not antigen-specific. In the Erk1/2 phosphorylation profiles, both CD8 alpha and beta genes increased the phosphorylation but the highest one was in the CD8αβ expressing TCR-NK cells.

The TCR used in this study was MHC-I restricted and targeted tyrosinase expressed by A375 cells thus we worked with CD8 co-receptor which is known to bind

MHC-I molecules. The effect of other co-receptor CD4 might be also investigated if it does have any effect on the cytotoxicity of TCR-NK cells. The combination of both co-receptors might be an interesting research subject. Moreover, the effect of the CD4 co-receptor might be investigated with an MHC-II restricted TCR.

The functions of CD8 dimers in T cells are still not fully clear and are being investigated by several studies (Cheroutre & Lambolez, 2008; Devine et al., 2000; My Bosselut et al., 2000; Zhong & Reinherz, 2005) . Even though there are lots of reports and studies about CD8αα and CD8αβ dimers, there is not enough information about the CD8ββ homodimer and how it functions in the TCR signalling. While there are many questions to be answered and signalling dynamics to be investigated, this study shows that the addition of CD8ββ and CD8αβ dimers increased the cytotoxic effects of TCR-NK cells. The detailed analyses of how these co-receptors aid TCR signalling dynamics are yet to be explored. On the other hand, the suppressor effects of CD8αα homodimer could be further explored. These findings provide advantageous information for further characterization and improvement of TCR-NK-based immunotherapies.

6. REFERENCES

Abel, A. M., C. Yang, M. S. Thakar and S. Malarkannan, "Natural Killer Cells: Development, Maturation, and Clinical Utilization", *Frontiers in Immunology*, Vol. 9, No. 9, pp. 1869-1881, 2018.

Alberts B., Johnson A. and Lewis J., 2002, "Molecular Biology of the Cell", 4th edition, *Garland Science*, Taylor and Francis Group, New York.

Armstrong, A. C., D. Eaton and J. C. Ewing, "Cellular immunotherapy for cancer", *British Medical Journal*, Vol. 323, No. 1, pp. 1289-1293, 2001.

Arruebo, M., N. Vilaboa, B. Sáez-Gutierrez, J. Lambea, A. Tres, M. Valladares and Á. González-Fernández, "Assessment of the Evolution of Cancer Treatment Therapies", *Cancers*, Vol. 3, No. 3, pp. 3279–3330, 2011.

Cheroutre, H., and F. Lambolez, "Doubting the TCR Coreceptor Function of CD8αα", *Immunity*, Vol. 28, No. 2, pp. 149–159, 2008.

Cohen, C. J., Y. F. Li, M. El-Gamil, P. F. Robbins, S. A. Rosenberg and R. A. Morgan, "Enhanced Antitumor Activity of T Cells Engineered to Express T-Cell Receptors with a Second Disulfide Bond", *Cancer Research*, Vol. 67, No. 8, pp. 3898–3903, 2007.

Cohen, C. J., Y. Zhao, Z. Zheng, S. A. Rosenberg and R. A. Morgan, "Enhanced Antitumor Activity of Murine-Human Hybrid T-Cell Receptor (TCR) in Human Lymphocytes Is Associated with Improved Pairing and TCR/CD3 Stability", *Cancer Research*, Vol. 66, No. 17, pp. 8878–8886, 2006.

Cooper, M. A., T. A. Fehniger and Caligiuri M.A., "The Biology of Human Natural Killer-Cell Subsets", *Trends in Immunology*, Vol. 22, No. 11, pp. 633-640, 2001.

Cooper, M. D., "Exploring lymphocyte differentiation pathways", *Immunological Reviews*, Vol. 185, No 1., pp. 175-185, 2002.

Dahlberg, C. I. M., D. Sarhan, M. Chrobok, A. D. Duru and E. Alici, "Natural Killer Cell-Based Therapies Targeting Cancer: Possible Strategies to Gain and Sustain Anti-Tumor Activity", *Frontiers in Immunology*, Vol. 6, No. 1, pp. 1-19, 2015.

Deftos, M. L., and M. J. Bevan, "Notch signaling in T cell development", *Current Opinion in Immunology*, Vol. 12, No. 1, pp. 166-172, 2000.

Desch, M. D., Y. R. Fernandez, J. Harrington, T. A. Livengood, D. A. Mendis, T. Northrup, H. U. Schmidt, S. L. Snowden, D. K. Yeomans, K. C. Garcia et al., "An αβ T Cell Receptor Structure at 2.5 A and Its Orientation in the TCR-MHC Complex", *Science*, Vol. 274, No. 1, pp. 209-219, 1996.

Devine, L., L. J. Kieffer, V. Aitken and P. B. Kavathas, "Human CD8β, But Not Mouse CD8β, Can Be Expressed in the Absence of CD8α as a ββ Homodimer", *The Journal of Immunology*, Vol. 164, No. 2, pp. 833-838, 2000.

Dobosz, P., and T. Dzieciatkowski, "The Intriguing History of Cancer Immuno therapy", *Frontiers in Immunology*, Vol. 10, No.1, pp. 2965, 2019.

Freeman, B. E., E. Hammarlund, H. P. Raué and M. K. Slifka, "Regulation of Innate CD8+ T-Cell Activation Mediated by Cytokines", *Proceedings of the National Academy of Sciences of the United States of America*, Vol. 109, No. 25, pp. 9971–9976, 2012.

Gascoigne, N. R. J., T. Zal, P. P. Yachi and J. A. H. Hoerter, "Co-Receptors and Recognition of Self at the Immunological Synapse", *Current Topics in Microbiology and Immunology*, Vol. 340, No. 1, pp. 171–189, 2010.

Gaud, G., R. Lesourne and P. E. Love, "Regulatory Mechanisms in T Cell Receptor Signalling", *Nature Reviews Immunology*, Vol. 18, No. 8, pp. 485–497, 2018.

Goding, S., Q. Yang, Z. Mi, P. D. Robbins and P. H. Basse, "Targeting of Products of Genes to Tumor Sites Using Adoptively Transferred A-NK and T-LAK Cells", *Cancer Gene Therapy*, Vol. 14, No. 5, pp. 441–450, 2007.

Golubovskaya, V., and L. Wu, "Different Subsets of T Cells, Memory, Effector Functions, and CAR-T Immunotherapy", *Cancers*, Vol. 8, No. 3, pp. 36-42, 2016.

Hayes, C., "Cellular Immunotherapies for Cancer", *Irish Journal of Medical Science*, Vol. 190, No. 1, pp. 41-57, 2021.

Herberman R.B., M.E. Nunn, and D. H. Lavrin, "Natural Cytotoxic Reactivity of Mouse Lymphoid Cells Against Syngeneic and Allogeneic Tumors I. Distribution of Reactivity and Specificity", *International Journal of Cancer*, Vol. 16, No. 2, pp. 216-229, 1975.

Hwang, J. R., Y. Byeon, D. Kim and S. G. Park, "Recent Insights of T Cell Receptor-Mediated Signaling Pathways for T Cell Activation and Development", *Experimental and Molecular Medicine*, Vol. 52, No. 5, pp. 750–761, 2020.

Janeway, C. A., and R. Medzhitov, "Innate Immune Recognition", *Annual Review of Immunology*, Vol. 20, No. 1, pp. 197–216, 2002.

Jensen, P. E., "Recent Advances in Antigen Processing and Presentation", *Nature Immunology*, Vol. 8, No. 10, pp. 1041–1048, 2007.

Karre, K., H. G. Ljunggren, G. Piontek and R. Kiessling, "Selective Rejection of H-2-Deficient Lymphoma Variants Suggests Alternative Immune Defence Strategy", *Nature*, Vol. 219, No. 6055, pp. 675-678, 1986.

Kern, P., R. E. Hussey, R. Spoerl, E. L. Reinherz and H. C. Chang, "Expression, Purification, and Functional Analysis of Murine Ectodomain Fragments of CD8αα and CD8αβ Dimers", *Journal of Biological Chemistry*, Vol. 274, No. 38, pp. 27237–27243, 1999.

Kershaw, M. H., J. A. Westwood and P. K. Darcy, "Gene-Engineered T Cells for Cancer Therapy", *Nature Reviews Cancer*, Vol. 13, No. 8, pp. 525–541, 2013.

Kiessling, R., E. Kiein, H. Wigzell, R. Kiessling' and E. Klein', ""Natural" killer cells in the mouse. II. Cytotoxic cells with specificity for mouse Moloney leukemia cells. Characteristics of the killer cell", *Eurepean Journal of Immunology*, Vol. 5, No. 2, pp. 117-121, 1975.

Klingemann, H., L. Boissel and F. Toneguzzo, "Natural Killer Cells for Immunotherapy - Advantages of the NK-92 Cell Line over Blood NK Cells", *Frontiers in Immunology*, Vol. 7, No. 1, p. 91, 2016.

Krzewski, K., and J. L. Strominger, "The Killer's Kiss: The Many Functions of NK Cell Immunological Synapses", *Current Opinion in Cell Biology*, Vol. 20, No. 5, pp. 597–605, 2008.

Kucuksezer, U. C., E. Aktas Cetin, F. Esen, I. Tahrali, N. Akdeniz, M. Y. Gelmez and G. Deniz, "The Role of Natural Killer Cells in Autoimmune Diseases", *Frontiers in Immunology*, Vol. 12, No.1, p. 622306, 2021.

Kumar, B. v., T. J. Connors and D. L. Farber, "Human T Cell Development, Localization, and Function throughout Life", *Immunity*, Vol. 48, No. 2, pp. 202–213, Cell Press, 2018.

Kupfer, A., and S. J. Singer, "The specific interaction of helper T cells and antigen-presenting B cells. IV. Membrane and cytoskeletal reorganizations in the bound T cell as a function of antigen dose", *The Journal of Experimental Medicine*, Vol. 170, No.5, pp. 1697-1713, 1989.

Lander, S., L. M. Linton, B. Birren, C. Nusbaum, M. C. Zody, J. Baldwin, K. Devon, K. Dewar, M. Doyle, W. FitzHugh et al., "Initial Sequencing and Analysis of the Human Genome International Human Genome Sequencing Consortium", *Nature*, Vol. 409, No. 6822, pp. 860-921, 2001.

Lin, Y., and H. Okada, "Cellular Immunotherapy for Malignant Gliomas", *Expert Opinion on Biological Therapy*, Vol. 16, No. 10, pp. 1265–1275, 2016.

Medzhitov, R., and C. Janeway, "Immunological Reviews Innate Immune Recognition: Mechanisms and Pathways", *Immunological Reviews*, Vol. 173, No. 1, pp. 89–97, 2000.

Medzhitov Ruslan, and Janeway CA, "Innate immunity: impact on the adaptive immune response", *Current Opinion in Immunology*, Vol. 9, No. 1, pp. 4-9, 1997.

Mensali, N., P. Dillard, M. Hebeisen, S. Lorenz, T. Theodossiou, M. R. Myhre, A. Fåne, G. Gaudernack, G. Kvalheim, J. H. Myklebust, E. M. Inderberg and S. Wälchli, "NK Cells Specifically TCR-Dressed to Kill Cancer Cells", *EBioMedicine*, Vol. 40, No. 1 , pp. 106–117, 2019.

Met, Ö., K. M. Jensen, C. A. Chamberlain, M. Donia and I. M. Svane, "Principles of Adoptive T Cell Therapy in Cancer", *Seminars in Immunopathology*, Vol. 41, No. 1, pp. 49–58, 2019.

Miller, J. F. A. P., "The discovery of thymus function and of thymus-derived lymphocytes", *Australia Immunological Reviews*, Vol. 185, No. 1, pp. 7–14, 2002.

Miller, M. J., S. H. Wei, I. Parker and M. D. Cahalan, "Two-Photon Imaging of Lymphocyte Motility and Antigen Response in Intact Lymph Node", *Science*, Vol. 296, No. 5574, pp. 1869–1873, 2002.

Mørch, A. M., Š. Bálint, A. M. Santos, S. J. Davis and M. L. Dustin, "Coreceptors and TCR Signaling – the Strong and the Weak of It", *Frontiers in Cell and Developmental Biology*, Vol. 8, No. 1, p. 597627 , 2020.

Morton, L. T., T. L. A. Wachsmann, M. H. Meeuwsen, A. K. Wouters, D. F. G. Remst, M. M. van Loenen, J. H. F. Falkenburg and M. H. M. Heemskerk, "T Cell Receptor Engineering of Primary NK Cells to Therapeutically Target Tumors and Tumor Immune Evasion", *Journal for Immunotherapy of Cancer*, Vol. 10, No. 3, p. e003715, 2022.

Müller, S., T. Bexte, V. Gebel, F. Kalensee, E. Stolzenberg, J. Hartmann, U. Koehl, A. Schambach, W. S. Wels, U. Modlich and E. Ullrich, "High Cytotoxic Efficiency of Lentivirally and Alpharetrovirally Engineered CD19-Specific Chimeric Antigen Receptor Natural Killer Cells Against Acute Lymphoblastic Leukemia", *Frontiers in Immunology*, Vol. 10, No. 1, p. 3123, 2020.

Murphy, K., Kenneth M., C. Weaver and C. Janeway, 2017, "Janeway's Immunobiology", 9th Edition, *Garland Science*, Taylor and Francis Group, New York.

My Bosselut, R., S. Kubo, T. Guinter, J. L. Kopacz, J. D. Altman, L. Feigenbaum and A. Singer, "Role of CD8β Domains in CD8 Coreceptor Function: Importance for MHC I Binding, Signaling, and Positive Selection of CD8+ T Cells in the Thymus", *Immunity*, Vol. 12, No. 4, pp. 409-418, 2000.

Neefjes, J., M. L. M. Jongsma, P. Paul and O. Bakke, "Towards a Systems Understanding of MHC Class I and MHC Class II Antigen Presentation", *Nature Reviews Immunology*, Vol. 11, No. 12, pp. 823–836, 2011.

Oiseth, S. J., and M. S. Aziz, "Cancer Immunotherapy: A Brief Review of the History, Possibilities, and Challenges Ahead", *Journal of Cancer Metastasis and Treatment*, Vol. 3, No. 10, pp. 250-261, 2017.

Okamoto, S., Y. Amaishi, Y. Goto, H. Ikeda, H. Fujiwara, K. Kuzushima, M. Yasukawa, H. Shiku and J. Mineno, "A Promising Vector for TCR Gene Therapy: Differential Effect of SiRNA, 2A Peptide, and Disulfide Bond on the Introduced TCR Expression", *Molecular Therapy - Nucleic Acids*, Vol. 1, No. 12, p. e63, 2012.

Orange, J. S., and Z. K. Ballas, "Natural Killer Cells in Human Health and Disease", *Clinical Immunology*, Vol. 118, No. 1, pp. 1–10, 2006.

Parlar, A., E. C. Sayitoglu, D. Ozkazanc, A. M. Georgoudaki, C. Pamukcu, M. Aras, B. J. Josey, M. Chrobok, S. Branecki, P. Zahedimaram, L. Ikromzoda, E. Alici, B. Erman, A. D. Duru and T. Sutlu, "Engineering Antigen-Specific NK Cell Lines against the Melanoma-Associated Antigen Tyrosinase via TCR Gene Transfer", *European Journal of Immunology*, Vol. 49, No. 8, pp. 1278–1290, 2019.

Paul, S., and G. Lal, "The Molecular Mechanism of Natural Killer Cells Function and Its Importance in Cancer Immunotherapy", *Frontiers in Immunology*, Vol. 8, No. 1, pp. 1124, 2017.

Pegram, H. J., M. H. Kershaw and P. K. Darcy, "Genetic Modification of Natural Killer Cells for Adoptive Cellular Immunotherapy", *Immunotherapy*, Vol. 1, No. 4, pp. 623–630, 2009.

Perica, K., J. C. Varela, M. Oelke and J. Schneck, "Adoptive T Cell Immunotherapy For Cancer", *Rambam Maimonides Medical Journal*, Vol. 6, No. 1, p. e0004, 2015.

Reeves, E., and E. James, "Antigen Processing and Immune Regulation in the Response to Tumours", *Immunology*, Vol. 150, No. 1, pp. 16–24, 2017.

Restifo, N. P., M. E. Dudley and S. A. Rosenberg, "Adoptive Immunotherapy for Cancer: Harnessing the T Cell Response", *Nature Reviews Immunology*, Vol. 12, No. 4, pp. 269–281, 2012.

Robey, E., and B. J. Fowlkes, "Selective Events in T Cell Development Further Annual Reviews", *Annual Review of Immunology*, Vol. 12, No.1, pp. 675-705, 1994.

Rolf Kiessling, B., G. Petranyi, K. Karre, M. Jondal, D. Tracey, H. Wigzell, G. Samaritan Hospital, M. Nunn, J. Y. Djeu, M. Glaser et al., "Killer Cells: A Functional Comparison Between Natural, Immune T-Cell and Antibody-dependent in vitro Systems", *The Journal of Experimental Medicine*, Vol. 143, No. 1, pp. 772-780, 1976.

Rossjohn, J., S. Gras, J. J. Miles, S. J. Turner, D. I. Godfrey and J. McCluskey, "T Cell Antigen Receptor Recognition of Antigen-Presenting Molecules", *Annual Review of Immunology*, Vol. 33, No. 1, pp. 169–200, 2015.

Samelson, L. E., R. D. Klausner,M Baniyash and P. Garcia-Morales, "The T-Cell Antigen Receptor Structure and Mechanism of Activation", *Advances in Neuroimmunology*, Vol. 540, No. 1, pp. 1-3, 1988.

Santana, M. A., and F. Esquivel-Guadarrama, "Cell Biology of T Cell Activation and Differentiation", *International Review of Cytology*, Vol. 250, No. 1, pp. 217–274, 2006.

Savas, P., R. Salgado, C. Denkert, C. Sotiriou, P. K. Darcy, M. J. Smyth and S. Loi, "Clinical Relevance of Host Immunity in Breast Cancer: From TILs to the Clinic", *Nature Reviews Clinical Oncology*, Vol. 13, No. 4, pp. 228–241, 2016.

Schilhamm, M. W., W.-P. Fung-Leung, A. RahemtuUa, T. KuendigA, L. Zhang, J. Potter, R. G. Miller, H. HengartnerA and T. W. Mak, "Alloreactive Cytotoxic T Cells Can Develop and Function in Mice Lacking Both CD4 and CD8", *European Journal of Immunology*, Vol. 23, No. 6, pp. 1299-1304, 1993.

Shah, K., A. Al-Haidari, J. Sun and J. U. Kazi, "T Cell Receptor (TCR) Signaling in Health and Disease", *Signal Transduction and Targeted Therapy*, Vol. 6, No. 1, p. 412, 2021.

Sharon, E., L. v. Sibener, A. Battle, H. B. Fraser, K. Christopher Garcia and J. K. Pritchard, "Genetic Variation in MHC Proteins Is Associated with T Cell Receptor Expression Biases", *Nature Genetics*, Vol. 48, No. 9, pp. 995–1002, 2016.

Singer, A., S. Adoro and J. H. Park, "Lineage Fate and Intense Debate: Myths, Models and Mechanisms of CD4- versus CD8-Lineage Choice", *Nature Reviews Immunology*, Vol. 8, No. 10, pp. 788–801, 2008.

Sivori, S., P. Vacca, G. del Zotto, E. Munari, M. C. Mingari and L. Moretta, "Human NK Cells: Surface Receptors, Inhibitory Checkpoints, and Translational Applications", *Cellular and Molecular Immunology*, Vol. 16, No. 5, pp. 430–441, 2019.

Smyth, M. J., E. Cretney, J. M. Kelly, J. A. Westwood, S. E. A. Street, H. Yagita, K. Takeda, S. L. H. V. Dommelen, M. A. Degli-Esposti and Y. Hayakawa, "Activation of NK Cell Cytotoxicity", *Molecular Immunology*, Vol. 42, No. 4, pp. 501–510, 2005.

Spada, F. M., Y. Koezuka and S. A. Porcelli, "CD1d-Restricted Recognition of Synthetic Glycolipid Antigens by Human Natural Killer T Cells", *Journal of Experimental Medicine*, Vol. 188, No. 8, pp. 1529-1534, 1998.

Sun, J. C., and L. L. Lanier, "NK Cell Development, Homeostasis and Function: Parallels with CD8 + T Cells", *Nature Reviews Immunology*, Vol. 11, No. 10, pp. 645–657, 2011.

Tam, Y. K., G. Maki, B. Miyagawa, B. Hennemann, T. Tonn and H.-G. Klingemann, "Characterization of Genetically Altered, Interleukin 2-Independent Natural Killer Cell Lines Suitable for Adoptive Cellular Immunotherapy", *Human Gene Therapy*, Vol. 10, No. 8, pp. 1359-1373, 1999.

Thome, J. J. C., N. Yudanin, Y. Ohmura, M. Kubota, B. Grinshpun, T. Sathaliyawala, T. Kato, H. Lerner, Y. Shen and D. L. Farber, "Spatial Map of Human t Cell Compartmentalization and Maintenance over Decades of Life", *Cell*, Vol. 159, No. 4, pp. 814–828, 2014.

Trapani, J. A., J. Davis, R. S. Vivien and M. J. Smyth, "Proapoptotic Functions of Cytotoxic Lymphocyte Granule Constituents in Vitro and in Vivo", *Current Opinion in Immunology*, Vol. 12, No. 3, pp. 323–329, 2000.

Trombetta, E. S., and I. Mellman, "Cell Biology of Antigen Processing in Vitro and in Vivo", *Annual Review of Immunology*, Vol. 23, No. 1 , pp. 975–1028, 2005.

Vacchelli, E., A. Eggermont, W. H. Fridman, J. Galon, E. Tartour, L. Zitvogel, G. Kroemer and L. Galluzzi, "Trial Watch Adoptive Cell Transfer for Anticancer Immunotherapy", *Oncoimmunology*, Vol. 2, No. 5, p. e24238, 2013.

Vivier, E., J. A. Nunè and F. Vély, "Natural Killer Cell Signaling Pathways", *Science*, Vol. 306, No. 5701, pp. 1517-1519, 2004.

Vivier, E., E. Tomasello, M. Baratin, T. Walzer and S. Ugolini, "Functions of Natural Killer Cells", *Nature Immunology*, Vol. 9, No. 5, pp. 503–510, 2008.

Vyas, J. M., A. G. van der Veen and H. L. Ploegh, "The Known Unknowns of Antigen Processing and Presentation", *Nature Reviews Immunology*, Vol. 8, No. 8, pp. 607–618, 2008.

Wong, W. K., J. Leem and J. Leem, "Comparative Analysis of the CDR Loops of Antigen Receptors", *Frontiers in Immunology*, Vol. 10, No. 1, p. 2454, 2019.

Wu, J., and L. L. Lanier, "Natural Killer Cells and Cancer", *Advances in Cancer Research*, Vol. 90, No. 1, pp. 127-156, 2003.

Xu, X., H. Li and C. Xu, "Structural Understanding of T Cell Receptor Triggering", *Cellular and Molecular Immunology*, Vol. 17, No. 3, pp. 193–202, 2020.

Zhang, J., Z. Tian, R. Sun, H. Wei and J. Zhang, "Characterization of interleukin-15 gene-modified human natural killer cells: Implications for adoptive cellular immunotherapy", *Haematologica*, Vol. 89, No. 3, pp. 338-347, 2004.

Zhong, W., and E. L. Reinherz, "CD8αα homodimer Expression and Role in CD8 T Cell Memory Generation During Influenza Virus A Infection in Mice", *European Journal of Immunology*, Vol. 35, No. 11, pp. 3103–3310, 2005.

APPENDIX A: Chemicals Used in This Study

Table A.1. Chemicals used in this study.

Chemicals and Media Components	Company
Acrylamide/Bis-acrylamide, 30% solution	Sigma, Germany
Agar	Sigma, Germany
Agarose	Sigma, Germany
Ammonium per sulphate	Sigma, Germany
Ampicillin	GellGro, USA
Boric Acid	Sigma, Germany
Bovine Serum Albumin (BSA)	Sigma, Germany
Brefeldin A	Biolegend, USA
Chloroquine	Sigma, Germany
DMEM	GIBCO, USA
DMSO	Sigma, Germany
DNA Gel Loading Dye, 6X	NEB, USA
DPBS	Sigma, Germany
EDTA	Applichem, Germany
Ethanol	Sigma, Germany
Ethidium Bromide	Sigma, Germany
Fetal Bovine Serum (FBS)	GIBCO, USA
HEPES Solution, 1M	Sigma, Germany
Interleukin-2	Proleukin, Novartis
Ionomycin from Streptomyces conglobatus	Sigma, Germany

Table A.1. Chemicals used in this study (cont.).

Isopropanol	Sigma, Germany
LB Broth	Sigma, Germany
L-glutamine, 200 mM	Sigma, Germany
MEM Vitamin Solution, 100X	GIBCO, USA
MEM Non-essential Amino Acid Solution	GIBCO, USA
2-Mercaptoethanol	Sigma, Germany
Methanol	Sigma, Germany
Monensin	Biolegend, USA
NaCl	Sigma, Germany
N,N,N′,N′Tetramethylethylenediamine	Sigma, Germany
(5Z)-7-Oxozeaenol	Sigma, Germany
Penicillin-Streptomycin	Sigma, Germany
PFA	Biolegend, USA
Phorbol 12-myristate 13-acetate (PMA)	Sigma, Germany
PIPES	Sigma, Germany
Protamine Sulfate	GIBCO, USA
RPMI-1640	Cytiva, UK
Saponin	Sigma, Germany
Sodium dodecyl sulphate	Sigma, Germany
Trizma	Sigma, Germany

APPENDIX B: Equipments Used in This Study

Table B.1. Equipments used in this study.

Equipment	**Company**
Autoclave	Astell Swiftclave, UK
Balance	Precisa BJ210C
Centrifuge	Beckman Coulter, Allegra X-12 , USA Beckman Coulter, Allegra X-30 R, USA
CO2 Incubator	Steri Cycle i60, Thermo Fisher Scientific, USA
Deepfreeze	-150°C, Thermo Fisher Scientific, USA -80 °C, Binder, USA -20°C, Bosch, Turkey
Electrophoresis Apparatus	Thermo Fisher Scientific, EC1000_90 PowerSuply, USA Thermo Fisher Scientific, MIDICELL PRIMO, USA
Filters (0.22 µm and 0.45 µm)	Molgen, Turkey
Flow Cytometer	BD FACSCalibur Flow Cytometer, USA BD Influx™ Cell Sorter, USA

Table B.1. Equipments used in this study (cont.).

Gel documentation	BIO-RAD, USA
Heater/Stirrer	Yellow Line, USA
Hemocytometer	ISOLAB, Germany
Ice Machine	Scotsman Inc., USA
Incubator	BINDER, USA
Laminar Flow	Thermo Fisher Scientific SDFE2020, USA
Liquid Nitrogen Tank	Taylor-Wharton, 3000RS, USA
Microliter Pipettes	Axygen, USA
Microscope	Zeiss, Primo Vert, Germany
Microcentrifuge	Beckman Coulter Microfuge 16, USA GILSON GmCLab Capsulfuge PMC-880, Mikro200R, Hetich, Germany
Microwave Oven	Beko, Turkey
pH meter	Hanna HI 2020 Edge®, USA
Refrigerator	Bosch, Turkey Arçelik, Turkey
Shaker Incubator	New Brunswick Sci., Innova 4330, USA
Spectrophotometer	Beckman Coulter DU730, USA NanodropTM 2000, Thermo Fisher Scientific, USA
Thermocycler	Eppendorf, Mastercycler Gradient, Germany
Thermoshaker	Thermal Shake Lite VWR, USA
Vortex	CliftonTM Cyclone Vortex Mixers, USA
Waterbath	Memmert Water Bath , Germany

APPENDIX C: ADAPTATIONS

- Figure 1.2, 1.3, 1.4, 1.5, 1.6, 1.7, 1.8 and 1.9 were created using BioRender.com.
- Figure 1.1 was adapted from "Stem Cell Differentiation from Bone Marrow" by BioRender.com (2022) and retrieved from https://app.biorender.com/biorender-templates.

APPENDIX D: DNA Ladder Used in This Study

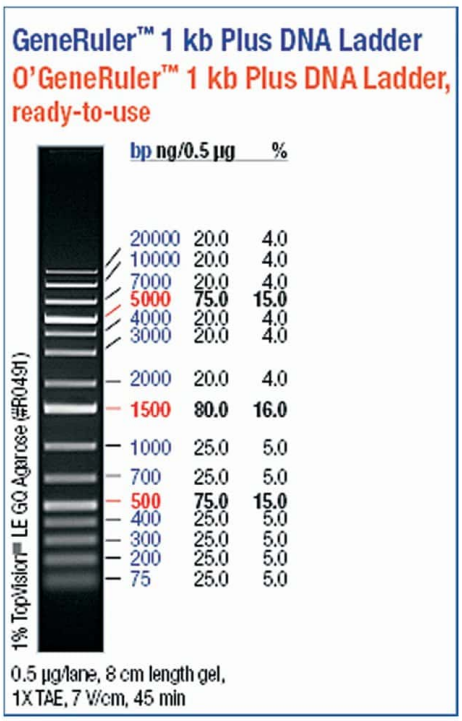

Figure D.1. DNA ladder used in this study.

APPENDIX E: Protein Ladder Used in This Study

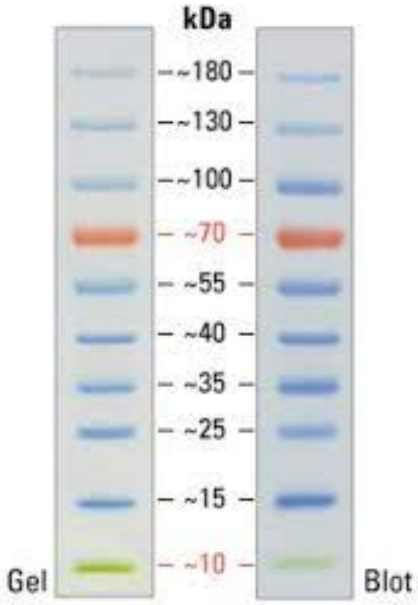

Figure E.1. Protein ladder used in this study.

APPENDIX F: Plasmid Maps

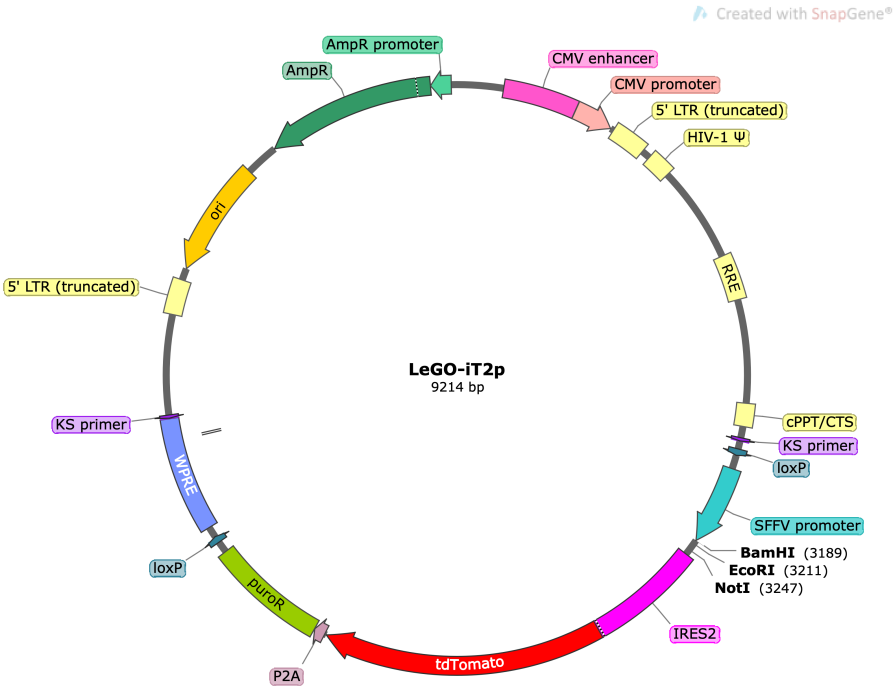

Figure F.1. The vector map of LeGO-iT2p.

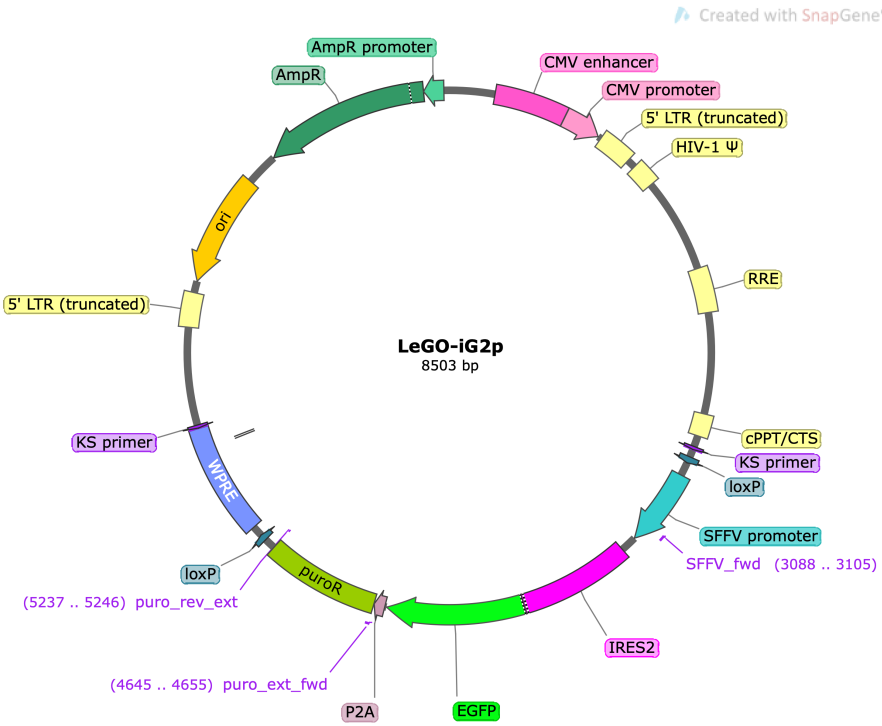

Figure F.2. The vector map of LeGO-iG2p.

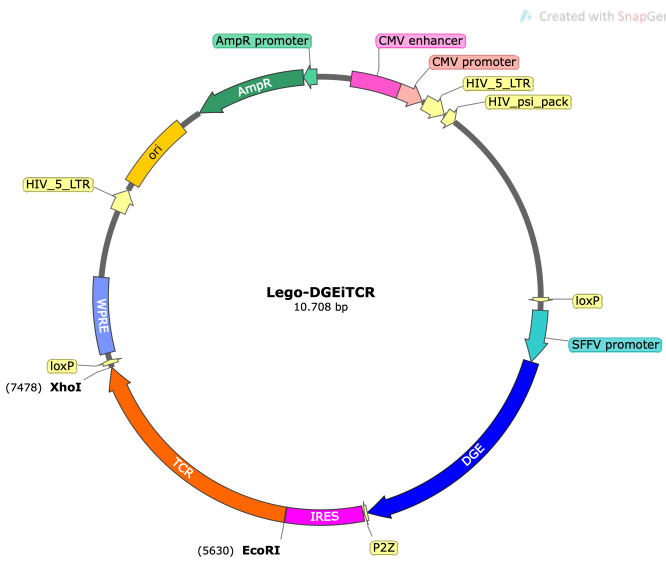

Figure F.3. The vector map of LeGO-DGEiTCR.

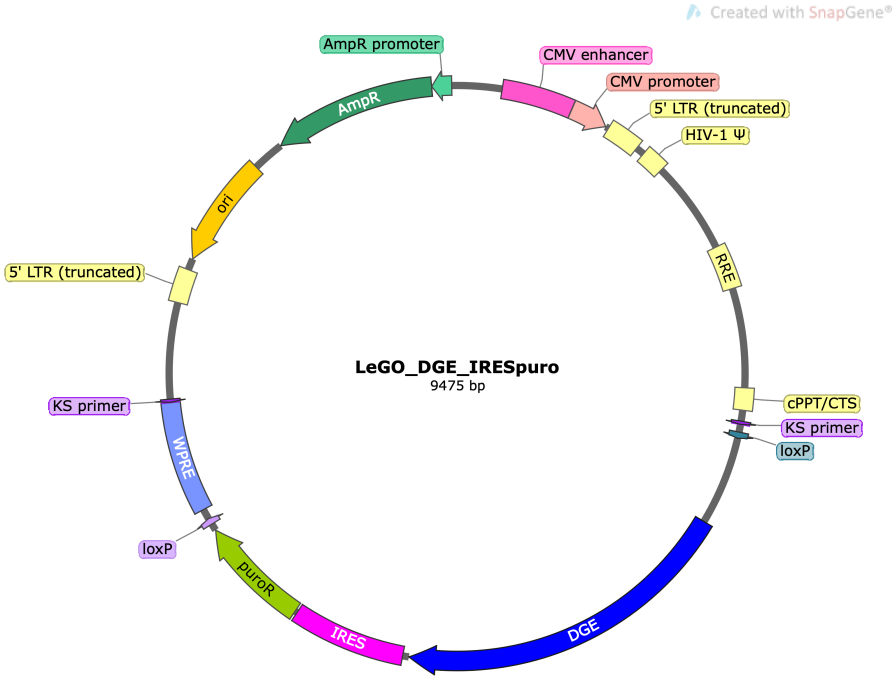

Figure F.4. The vector map of LeGO-DGE-IRESpuro.

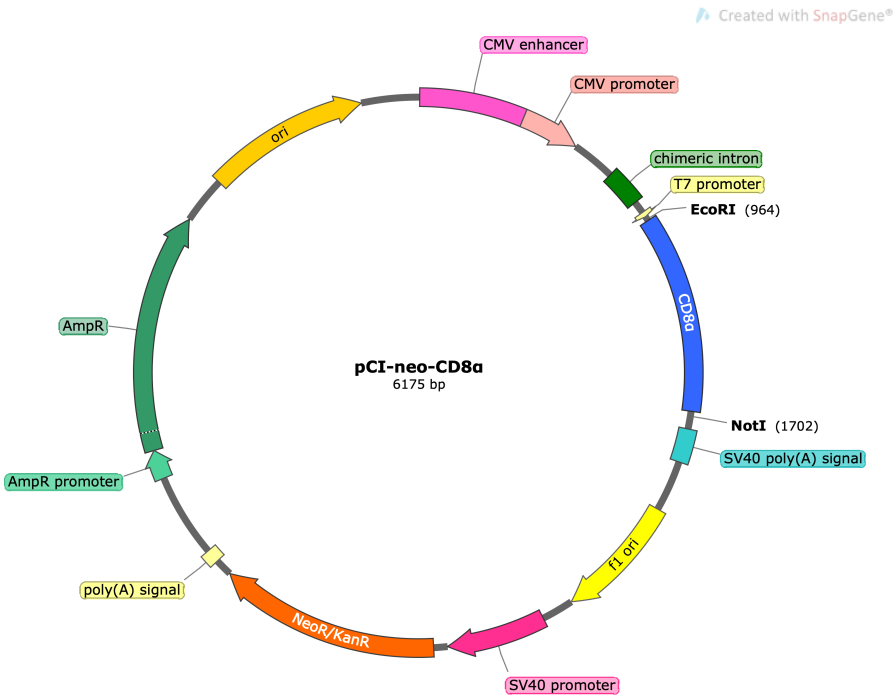

Figure F.5. The vector map of pCI-neo-CD8α

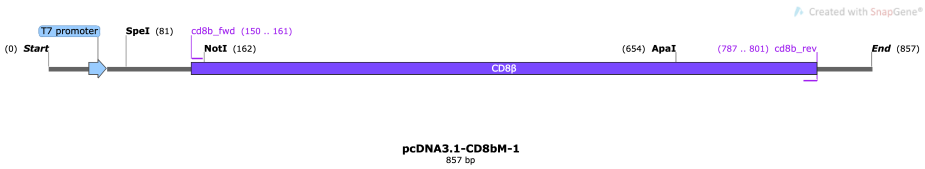

Figure F.6. The vector map of pcDNA3.1-CD8βM-1.

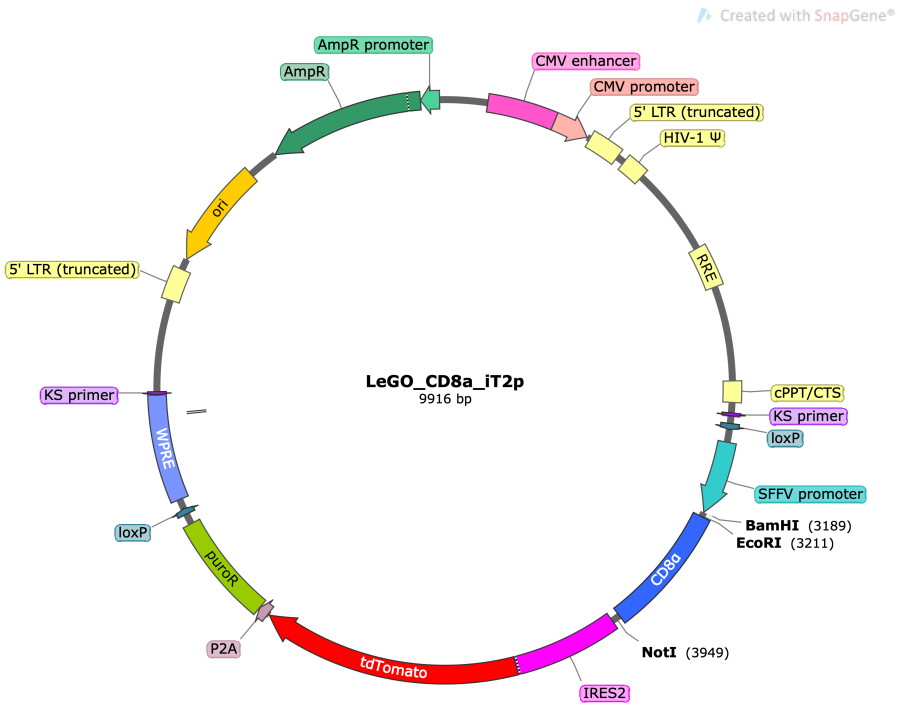

Figure F.7. The vector map of LeGO_CD8α_iT2p.

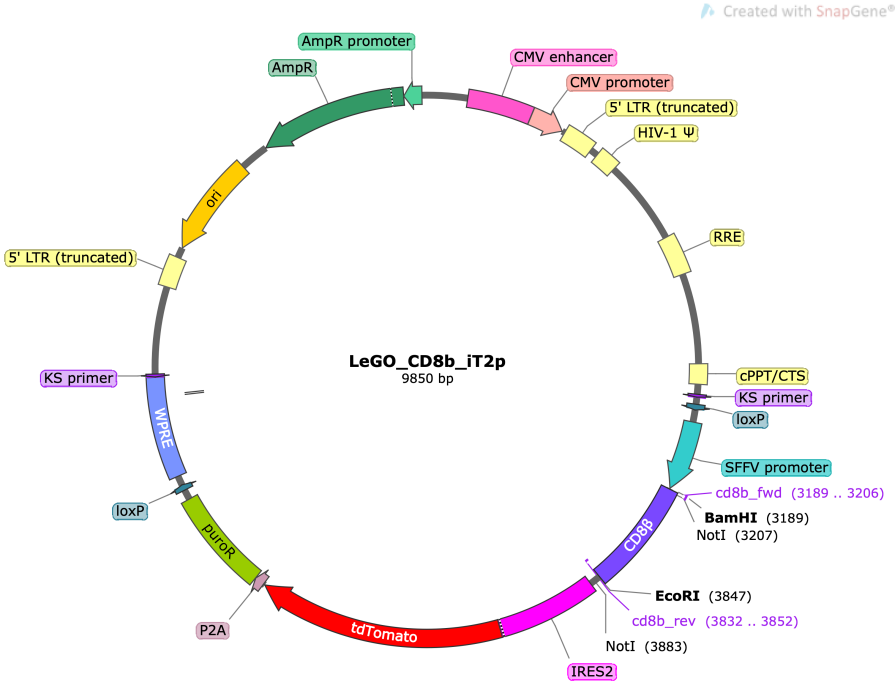

Figure F.8. The vector map of LeGO_CD8β_iT2p.

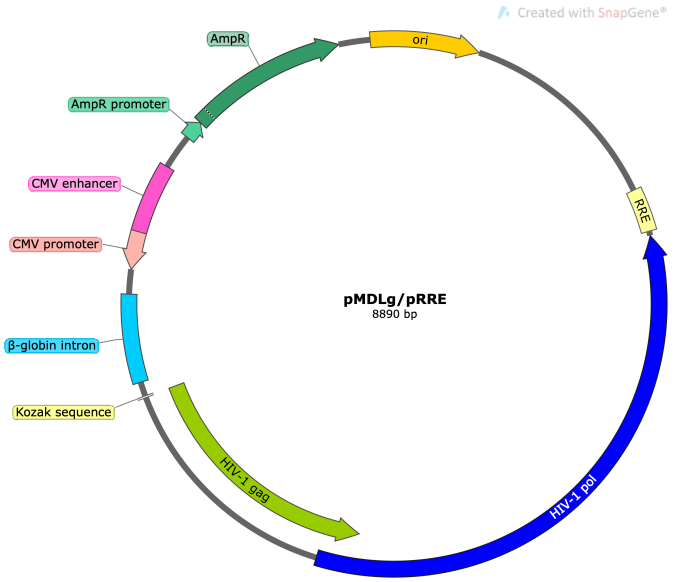

Figure F.9. The vector map of pMDLg/pRRE

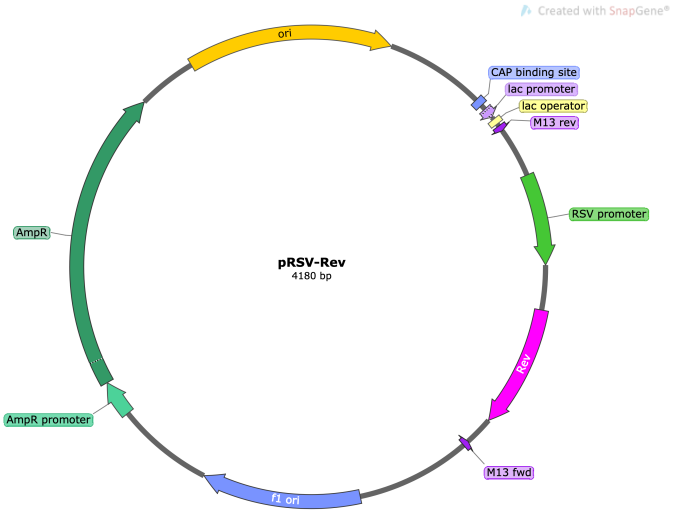

Figure F.10. The vector map of pRSV-Rev.

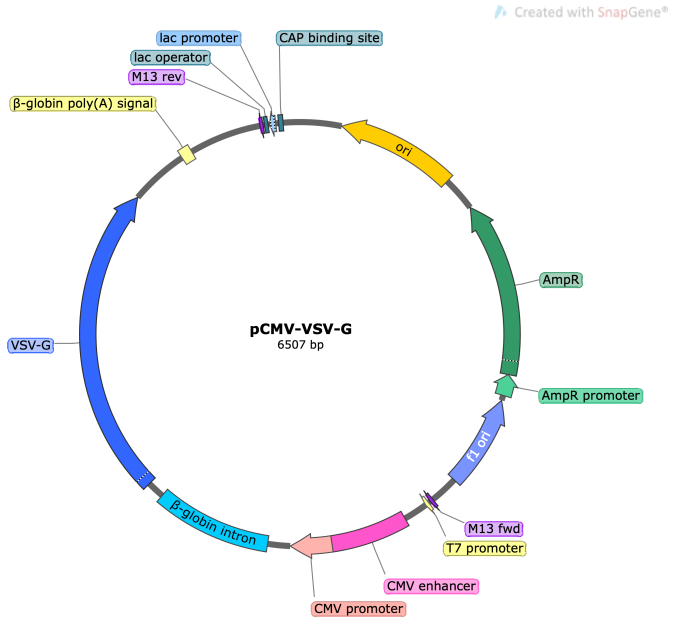

Figure F.11. The vector map of pCMV-VSV-G.